

Atomtronics

(Benasque Science Center, May 19 - Jun 01, 2024)

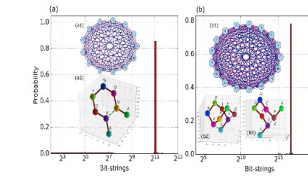
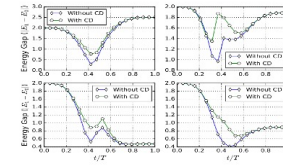
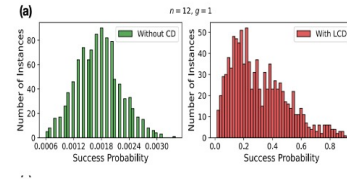
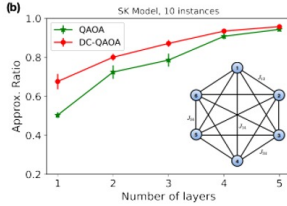
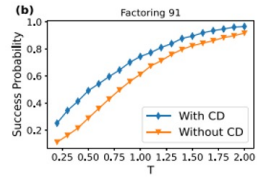
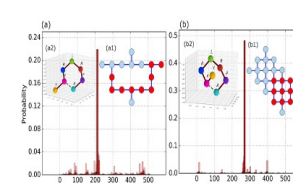
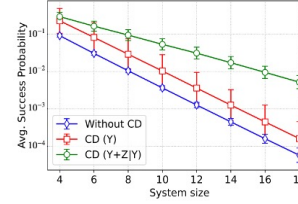
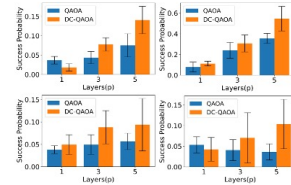
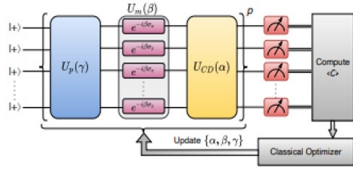
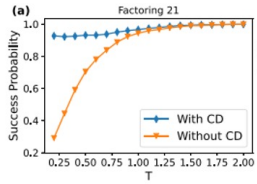
Fast transport and splitting of spin-orbit-coupled spin-1 BECs

Xi Chen

University of the Basque Country, UPV/EHU



Quantum Control & Quantum Optics Group @



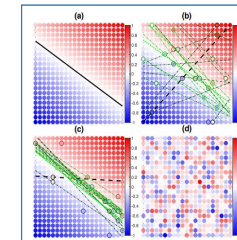
PRA 104, L050403 (2021)

PRR 4, 013141 (2022)

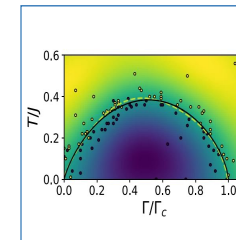
PRR 4, 043204 (2022)

PRR 4, L042030 (2022)

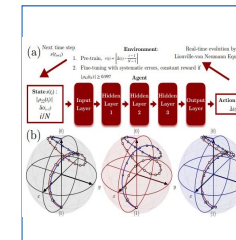
PR Applied 20, 014024 (2023)



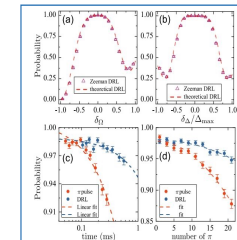
PRL 124, 140504 (2020)



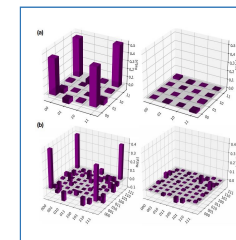
PRR 4, 013213 (2022)



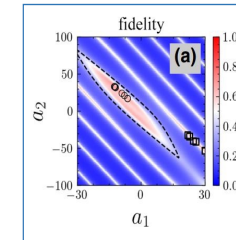
PRA 101, L040401 (2021)



SCPMA 65, 250312 (2022)



PR Applied 15, 024038 (2021)



PR Applied 17, 024040 (2022)

OUTLINE

1. Introduction

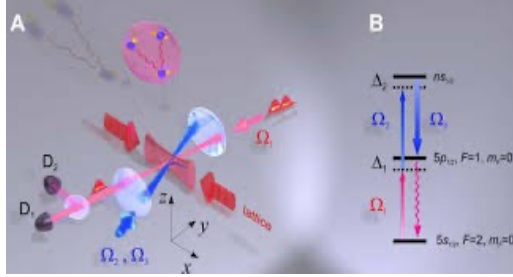
2. Trap Expansion

3. SOC Spin-1 BECs

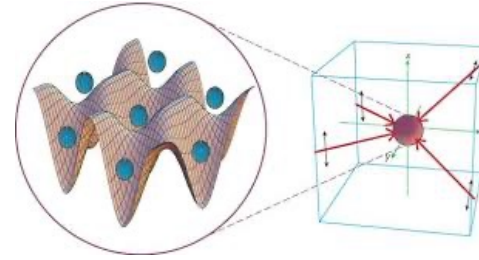
4. Application to cQED

5. Conclusion & Outlook

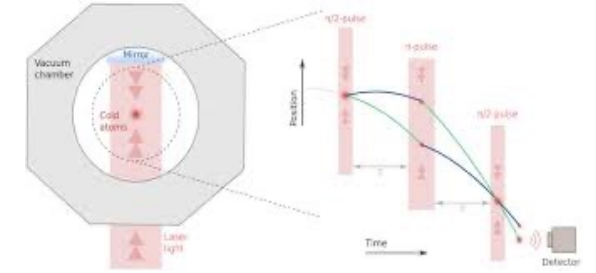
Quantum Information Processing



Quantum Simulation



Quantum Metrology



Essential: Preparation, control and manipulation of quantum states with high-fidelity and in a fast and robust way



Shortcuts To Adiabaticity

PHYSICAL REVIEW LETTERS

Highlights Recent Accepted Collections Authors Referees Search Press About Staff

Fast Optimal Frictionless Atom Cooling in Harmonic Traps: Shortcut to Adiabaticity

Xi Chen, A. Ruschhaupt, S. Schmidt, A. del Campo, D. Guéry-Odelin, and J. G. Muga
 Phys. Rev. Lett. **104**, 063002 – Published 11 February 2010



Article References Citing Articles (394) PDF HTML Export Citation

(a) Inverse engineering

(b) Transitionless quantum driving (counter-diabatic protocols)

REVIEWS OF MODERN PHYSICS, VOLUME 91, OCTOBER-DECEMBER 2019
Shortcuts to adiabaticity: Concepts, methods, and applications

D. Guéry-Odelin
 Laboratoire de Collisions Agrégats Réactivité, CNRS UMR 5589, IRSAMC,
 Université de Toulouse (UPS), 118 Route de Narbonne,
 31062 Toulouse CEDEX 4, France

A. Ruschhaupt and A. Kiely
 Department of Physics, University College Cork, Cork, Ireland

E. Torrontegui
 Instituto de Física Fundamental IFF-CSIC, Calle Serrano 113b, 28006 Madrid, Spain

S. Martínez-Garaot and J. G. Muga
 Departamento de Química Física, UPV/EHU, Apdo. 644, 48980 Bilbao, Spain

(published 24 October 2019)

Shortcuts to adiabaticity (STA) are fast routes to the final results of slow, adiabatic changes of the controlling parameters of a system. The shortcuts are designed by a set of analytical and numerical methods suitable for different systems and conditions. A motivation to apply STA methods to quantum systems is to manipulate them on timescales shorter than decoherence times. These shortcuts to adiabaticity have become instrumental in preparing and driving internal and motional states in atomic, molecular, and solid-state physics. Applications range from information transfer and processing based on gates or analog paradigms to interferometry and metrology. The multiplicity of STA paths for the controlling parameters may be used to enhance robustness versus noise and perturbations or to optimize relevant variables. Since adiabaticity is a widespread phenomenon, STA methods also extended beyond the quantum world to optical devices, classical mechanical systems, and statistical physics. Shortcuts to adiabaticity combine well with other concepts and techniques, in particular, with optimal control theory, and pose fundamental scientific and engineering questions such as finding speed limits, quantifying the third law, or determining process energy costs and efficiencies. Concepts, methods, and applications of shortcuts to adiabaticity are reviewed and promising prospects are outlined, as well as open questions and challenges ahead.

DOI: 10.1103/RevModPhys.91.045001

CONTENTS

I. Introduction	2	2. Examples of invariant-based inverse engineering	13
A. Overview of shortcuts to adiabaticity	2	a. Two-level system	13
B. Motivation and scope of this review	3	b. Lewis-Lesh family	14
II. Methods	4	3. Scaling laws	15
A. Overview of inverse engineering approaches	4	4. Connection with Lax pairs	16
1. Quantum transport	5	D. Variational methods	16
2. Spin manipulation	5	E. Fast forward	17
3. Beyond mean values	5	1. The original formalism	17
B. Counterdiabatic driving	6	2. Streamlined fast-forward approach	18
1. Superadiabatic iterations	8	3. Generalizations and terminology	19
2. Beyond the basic formalism	9	F. FAQUAD and related approaches	19
a. "Physical" unitary transformations	9	G. Optimal control and shortcuts to adiabaticity	20
b. Schemes that focus on one state	10	H. Robustness	21
c. Effective counterdiabatic field	10	1. Error sensitivity and its optimization using perturbation theory	21
d. Dressed-states approach	10	a. Illustrative example: Control of a two-level system	21
e. Variational approach	11	b. Optimization using perturbation theory in other settings	22
f. Counterdiabatic Born-Oppenheimer dynamics	12	2. Other approaches	23
g. Constant CD-term approximation	12	1. Three-level systems	23
C. Invariants and scaling laws	12		
1. Lewis-Riesenfeld invariants	12		

0034-6881/2019/91(4)/045001(54)

045001-1

© 2019 American Physical Society

RMP 91, 045001 (2019)

PHILOSOPHICAL TRANSACTIONS OF THE ROYAL SOCIETY A

MATHEMATICAL, PHYSICAL AND ENGINEERING SCIENCES

Shortcuts to adiabaticity: theoretical, experimental and interdisciplinary perspectives

Theme issue compiled and edited by Mikio Nakahara, Xi Chen, Yue Ban and Shumpei Masuda

Published 7 November 2022. Available online and in print.



Techniques of Shortcuts To Adiabaticity

(a) Inverse engineering

PRL 104, 063002 (2010); J. Phys. B: At. Mol. Opt. Phys. 42 241001 (2009)

(b) Transitionless quantum driving (counter-diabatic protocols)

J Phys. Chem. A107, 9937 (2003); J. Phys. A 42, 365303 (2009); PRL 105, 123003 (2010); 111, 100502 (2013)

(c) Fast-forward scaling approach

Proc. R. Soc. A 466, 1135 (2010); Phys. Rev. A 78, 062108 (2008)

(d) Rapid-scan approach

PRL 110, 240501 (2013)

(e) Time-scaled dynamics for STA

PR Research 2, 013133 (2020)

(f) Lax Pair from Classical Nonlinear Integrable Systems to Quantum

PRL 117, 070401 (2016)

Enhanced STA, Optimal control theory and so on



Implementation of STA in Harmonic Trap

Fast Optimal Frictionless Atom Cooling in Harmonic Traps: Shortcut to Adiabaticity

Xi Chen,^{1,2} A. Ruschhaupt,³ S. Schmidt,³ A. del Campo,⁴ D. Guéry-Odelin,⁵ and J. G. Muga¹

¹Departamento de Química-Física, UPV-EHU, Apartado 644, 48080 Bilbao, Spain

²Department of Physics, Shanghai University, 200444 Shanghai, People's Republic of China

experiments based on/or relevant to our STA proposals:

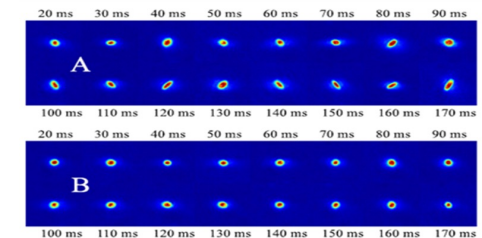
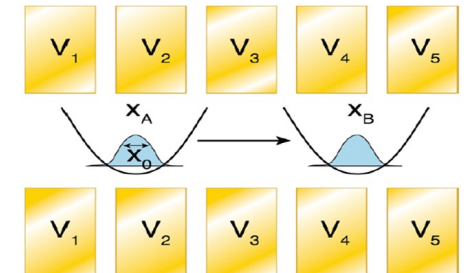
G. Labeyrie: Phys. Rev. A 82, 033430 (2010); EPL 93, 23001 (2011) Decompression of cold atoms

J. Schmiedmayer: Sci. Rep. 5, 10506 (2015). Compression of a quasicondensate

D. J. Wineland: Phys. Rev. Lett. 109, 080502 (2012) Ion transport

Haibing Wu: PRA 97, 013628; Science advances, 4 eaar5909 (2018) Fermi gas

Kim: Nat. Commun. 7, 12999 (2016) 171Yb^+ ion transport in phase space via shortcut to adiabaticity



Two/Three Level Quantum Systems

E. Arimondo & O. Morsch: Nat. Phys. 8, 147 (2012) [Accelerated optical lattice](#)

D. Suter: Phys. Rev. Lett. 110, 240501 (2013) [Nitrogen-vacancy centers spin](#)

D. D. Awschalom: Nat. Phys. 13, 330 (2017) [Nitrogen-vacancy centers spin](#)

G. S. Paraoanu: Science advances 5(2), eaau5999 (2019) [Transmon circuit](#)

Dapeng Yu: Phys. Rev. Lett. 122, 080501 (2019) [Superconducting qubit](#)

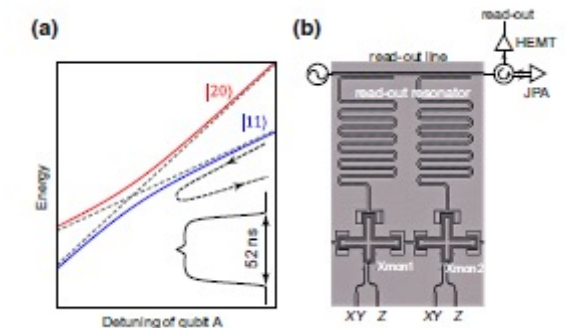
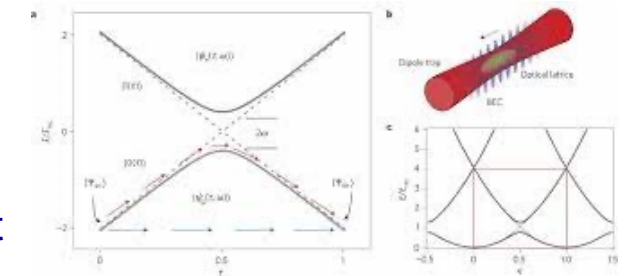
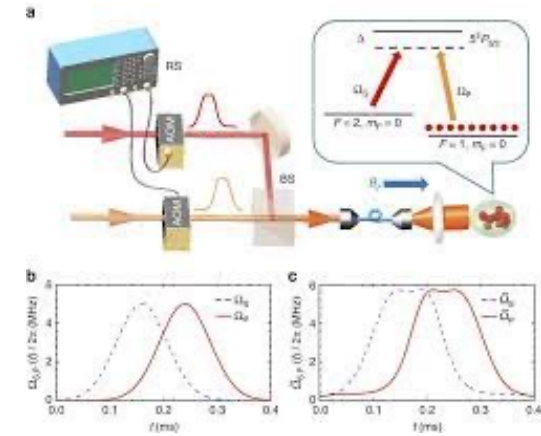
Yi Ying: New J. Phys. 20 065003 (2018); Phys. Rev. Applied 11, 034030 (2019) [Xmon qubit](#)

Xi Chen, Hui Yan and Shiliang Zhu: Nature Commun. 7, 12479 (2016). STIRAP [Cold atoms](#)

Xinhua Peng: Phys. Rev. Appl. 13, 044059 (2020) [Spin chain](#)

Y. Yan, **Xi Chen**, and S. Kröll, npj Quantum information 7, 138 (2021) [rare-earth ion](#)

Akira Oiwa: Phys. Rev. Lett. 132, 027002 (2024) [quantum dot](#)



Shortcuts to Adiabaticity for Other Fields

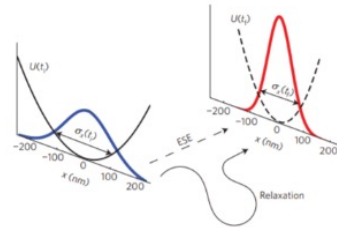
Statistical Physics



Engineered swift equilibration of a Brownian particle

Ignacio A. Martínez¹, Artyom Petrosyan¹, David Guéry-Odelin², Emmanuel Trizac³ and Sergio Ciliberto^{1*}

A fundamental and intrinsic property of any device or natural system is its relaxation time τ_{relax} which is the time it takes to return to equilibrium after the sudden change of a control parameter¹. Reducing τ_{relax} is frequently necessary, and is often obtained by a complex feedback process. To overcome the limitations of such an approach, alternative methods based on suitable driving protocols have been recently demonstrated^{2,3}, for isolated quantum and classical systems^{4,5}. Their extension to open systems in contact with a thermostat is a stumbling block for applications. Here, we design a protocol, named Engineered Swift Equilibration (ESE), that shortcuts time-consuming relaxations, and we apply it to a Brownian particle trapped in an optical potential whose properties can be controlled in time. We implement the process experimentally, showing that it allows the system to reach equilibrium 100 times faster than the natural equilibration



Biology

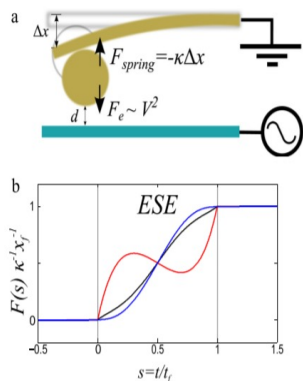


Controlling the speed and trajectory of evolution with counterdiabatic driving

Shamreen Iram^{1,7}, Emily Dolson^{2,7}, Joshua Chiel^{1,7}, Julia Pelesko^{1,2}, Nikhil Krishnan^{2,3}, Özenç Güngör¹, Benjamin Kuznets-Speck^{1,4}, Sebastian Deffner⁵, Efe Ilker⁶, Jacob G. Scott^{1,2,3} and Michael Hinczewski^{1,8}

The pace and unpredictability of evolution are critically relevant in a variety of modern challenges, such as combating drug resistance in pathogens and cancer, understanding how species respond to environmental perturbations like climate change and developing artificial selection approaches for agriculture. Great progress has been made in quantitative modelling of evolution using fitness landscapes, allowing a degree of prediction for future evolutionary histories. Yet fine-grained control of the speed and distributions of these trajectories remains elusive. We propose an approach to achieve this using ideas originally developed in a completely different context—counterdiabatic driving to control the behaviour of quantum states for applications like quantum computing and manipulating ultracold atoms. Implementing these ideas for the first time in a biological context, we show how a set of external control parameters (that is, varying drug concentrations and types, temperature and nutrients) can guide the probability distribution of genotypes in a population along a specified path and time interval. This level of control, allowing empirical optimization of evolutionary speed and trajectories, has myriad potential applications, from enhancing adaptive therapies for diseases to the development of thermotolerant crops in preparation for climate change, to accelerating bioengineering methods built on evolutionary models, like directed evolution of biomolecules.

Low Dimensional System



APPLIED PHYSICS LETTERS 109, 113502 (2016)

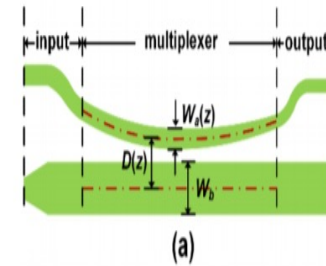
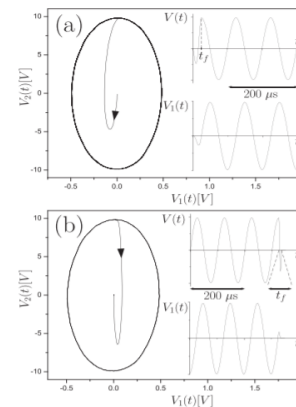
Fast equilibrium switch of a micro mechanical oscillator

Anne Le Cunuder,¹ Ignacio A. Martínez,¹ Artyom Petrosyan,¹ David Guéry-Odelin,² Emmanuel Trizac,³ and Sergio Ciliberto^{1,*}
¹Université de Lyon, CNRS, Laboratoire de Physique de l'École Normale Supérieure, UMR5672, 46 Allée d'Italie, 69364 Lyon, France
²Laboratoire de Collisions Agrégats Réactivité, CNRS UMR 5589, IRSAMC, Toulouse, France
³LPTMS, CNRS, Univ. Paris-Sud, Université Paris-Saclay, 91405 Orsay, France

(Received 6 June 2016; accepted 2 September 2016; published online 16 September 2016)

We demonstrate an accurate method to control the motion of a micromechanical oscillator in contact with a thermal bath. The experiment is carried out on the cantilever tip of an atomic force microscope. Applying an appropriate time dependent external force, we decrease the time necessary to reach equilibrium by two orders of magnitude compared to the intrinsic equilibration time. Finally, we analyze the energetic cost of such a fast equilibration, by measuring with $k_B T$ accuracy the energy exchanges along the process. Published by AIP Publishing. [http://dx.doi.org/10.1063/1.4962825]

Classical Physics (RC circuit; Crane; Waveguide; Polarizer)



Silicon mode (de)multiplexers with parameters optimized using shortcuts to adiabaticity

DEFEN GUO^{1,3} AND TAO CHU^{1,2,*}

¹Institute of Semiconductors, Chinese Academy of Sciences, P.O. Box 912, Beijing 100083, China
²College of Information Science and Electronic Engineering, Zhejiang University, 38 Zheda Road, Hangzhou 310027, China
³University of Chinese Academy of Sciences, 19 A Yuquan Rd, Shijingshan District, Beijing 100049, China
 *chutao@zju.edu.cn

Fig. 1. Schematic diagrams of the optimized mode (de)multiplexer using STA. (a) Top view. (b) Side view.

OUTLINE

1. Introduction

2. Trap Expansion

3. SOC Spin-1 BECs

4. Application to cQED

5. Conclusion & Outlook

Frictionless Atom Cooling in Harmonic Trap

PRL 104, 063002 (2010)

Hamiltonian

$$H = \hat{p}^2 / 2m + m\omega(t)^2 \hat{q}^2 / 2$$

Invariant

$$I(t) = 1/2[(1/b^2)\hat{q}^2 m\omega_0^2 + \frac{1}{m}\hat{\pi}^2]$$

$$\hat{\pi} = b(t)\hat{p} - m\dot{b}\hat{q} \text{ conjugate to } \hat{q}/b$$

$$\frac{dI}{dt} \equiv 0$$



$$\ddot{b} + \omega(t)^2 b = \omega_0^2 / b^3$$

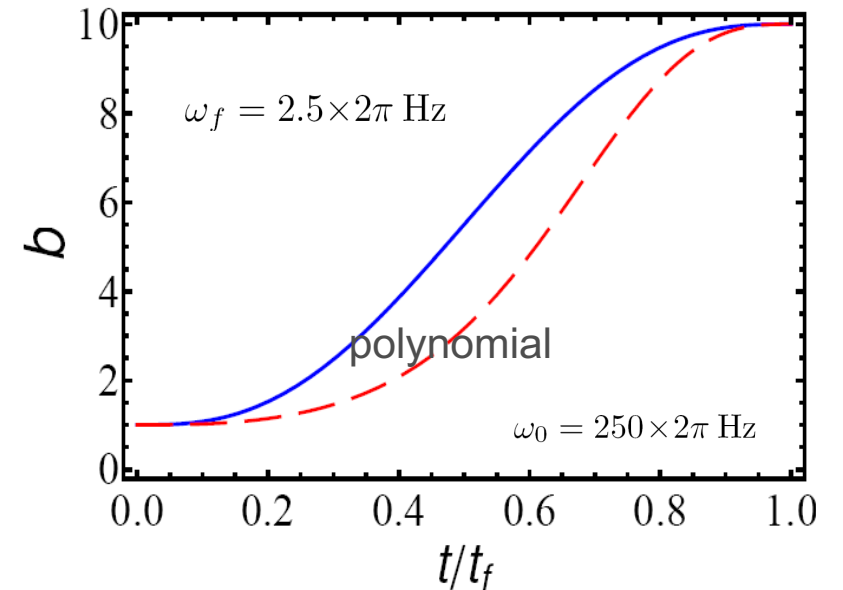
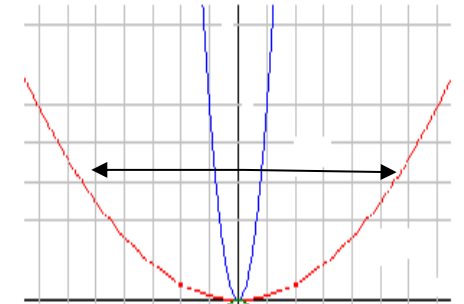
In general the state is a superposition of “expanding modes”

$$\psi(t, x) = \sum_n c_n \underbrace{e^{i\alpha_n(t)} \langle x | n(t) \rangle}_{\Psi_n(t, x)}$$

$$\alpha_n(t) = -(n + 1/2)\omega_0 \int_0^t dt' / b^2$$



Ermakov equation



Scaling law and Self-similarity

Time-dependent Gross-Pitaevskii equation

$$i\hbar \frac{\partial \psi}{\partial t} = \left[-\frac{\hbar^2}{2m} \frac{\partial^2}{\partial x^2} + \frac{1}{2} m \omega(t)^2 x^2 + g |\psi|^2 \right] \psi$$

With self-similar dynamics

$$\psi(x, t) = b^{-1/2} e^{i \frac{m}{2\hbar} \frac{b}{b} x^2} e^{-i E_n \tau(t) / \hbar} \Psi_n(x/b, 0)$$

Solution of the Ermakov equation: scaling factor

$$\ddot{b} + \omega(t)^2 b = \frac{\omega_0^2}{b^3}$$

which makes the wave function satisfies

$$i\hbar \frac{\partial \Psi}{\partial \tau} = -\frac{\hbar^2}{2m} \frac{\partial^2 \Psi}{\partial \rho^2} + \frac{m \omega_0^2}{2} \rho^2 \Psi + g b |\Psi|^2 \Psi$$

$$\tau(t) = \int_0^t \frac{dt'}{b^2}$$

The condition is required:

- (1) time-dependent $g(t)$ $g(t) = g_0/b(t)$
- (2) Thomas-Fermi limit

$$\ddot{b} + \omega(t)^2 b = \frac{\omega_0^2}{b^2}, \quad \tau(t) = \int_0^t \frac{dt'}{b}$$

JPB 42, 241001 (2009)
 PRA 84, 031606 (2011)
 PRX 4, 021013 (2014)
 PRL 77, 5315 (1996)
 NJP 12, 113005 (2010)

These results are applicable to trapped BECs, TG gas and Fermi gas.

Variational approach for STA

Time-dependent 1-D GP equation with harmonic potential

Lagrange density

$$\mathcal{L} = \frac{i}{2} \left(\psi \frac{\partial \psi^*}{\partial t} - \psi^* \frac{\partial \psi}{\partial t} \right) - \frac{1}{2} \left| \frac{\partial \psi}{\partial x} \right|^2 - \frac{1}{2} \omega^2(t) x^2 |\psi|^2 - \frac{1}{2} gN |\psi|^4.$$

Chaos 30, 053131 (2020)

By choosing Gaussian ansatz

$$\psi(x, t) = A(t) \exp \left[-\frac{x^2}{2a^2(t)} + ib(t)x^2 \right]$$

The variational approach gives the following differential equation:

$$\ddot{a} + \omega^2(t)a = \frac{1}{a^3} + \frac{gN}{\sqrt{2\pi} a^2}$$

PRL 77, 5320 (1996); PRL 83, 1715 (1999)

Nolinear Optics, B. A. Malomed, Progress in Optics 43, 71 (2002)

This allows us to study the case of weakly interaction, except for $g=0$ or $g=\infty$

Also applicable to other scenario: Frequency-Tunable Transmon Superconducting Qubits

$$\hat{H}_T \simeq 4E_C \hat{n}^2 + \frac{1}{2} E_J \hat{\varphi}^2 - \frac{1}{24} E_J \hat{\varphi}^4$$

nonlinear harmonic oscillator : J.J. García-Ripoll et. al. PR Appl. 14, 044035 (2020)

Perturbed Kepler-problem

analogous to fictitious classical particle with unit mass

$$\ddot{a} + \omega^2(t)a = \frac{1}{a^3} + \frac{gN}{\sqrt{2\pi}a^2}$$



$$U(a) = \frac{1}{2}\omega^2(t)a^2 + \frac{1}{2a^2} + \frac{gN}{\sqrt{2\pi}a}$$

$$\mathcal{E}(a) = \frac{\dot{a}^2}{2} + \frac{1}{2}\omega^2(t)a^2 + \frac{1}{2a^2} + \frac{gN}{\sqrt{2\pi}a}$$

$$\partial U / \partial a = 0$$

at 0 and t_f



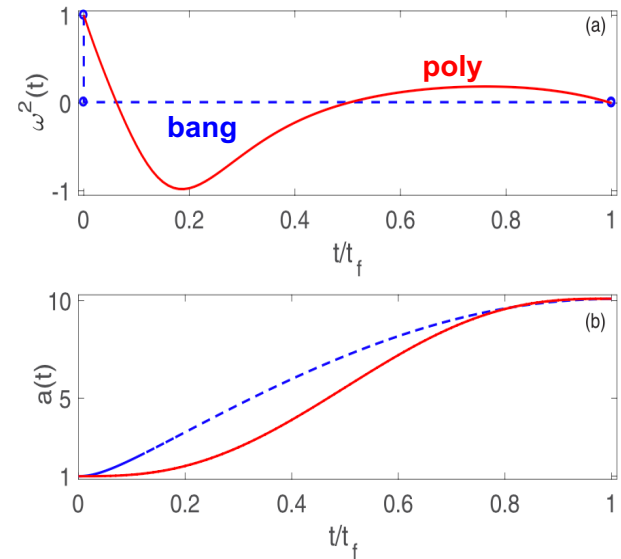
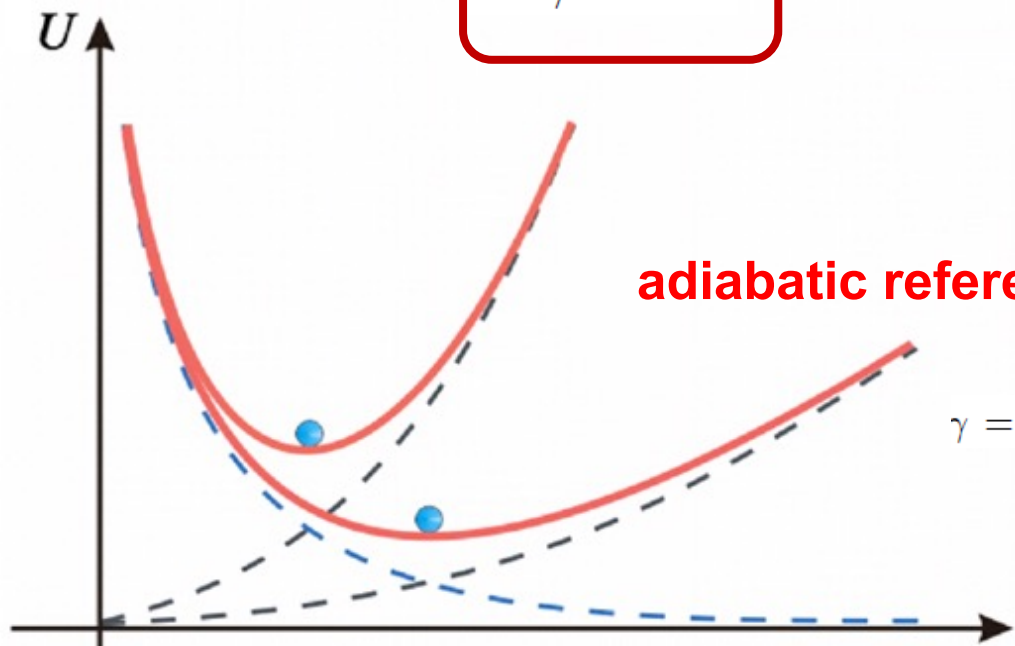
$$a_i^4 + \frac{gN}{\sqrt{2\pi}}a_i^2 = 1,$$

$$\gamma^4 a_f^4 + \frac{gN}{\sqrt{2\pi}}a_f^2 = 1$$

$$a(0) = a_i, a(t_f) = a_f,$$

$$\dot{a}(0) = \dot{a}(t_f) = 0,$$

$$\ddot{a}(0) = \ddot{a}(t_f) = 0,$$

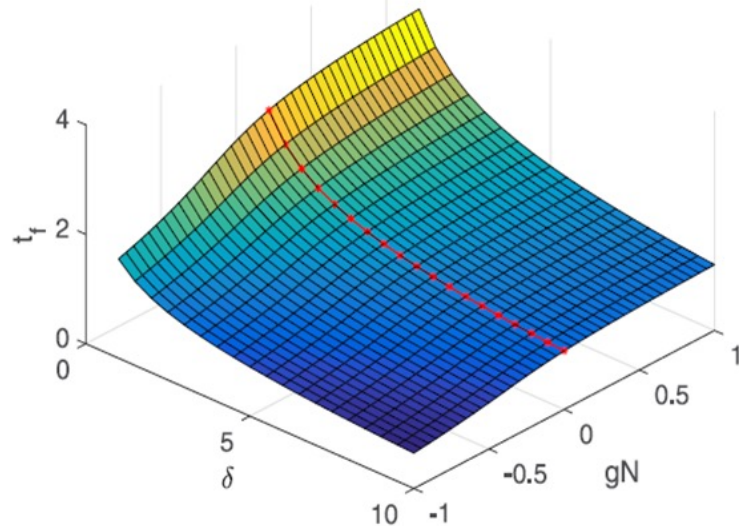
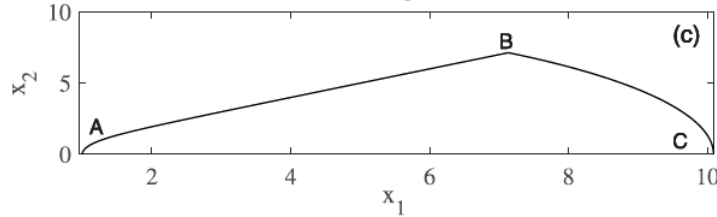
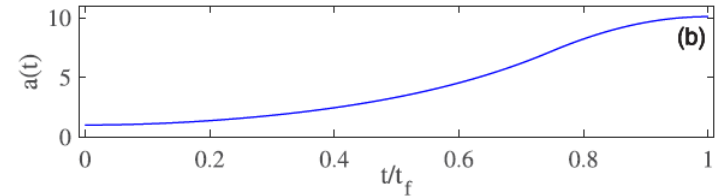
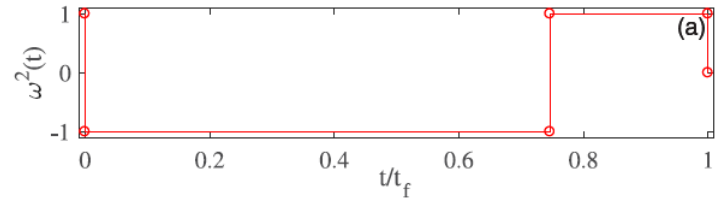


these boundary conditions imply the minimization of energy, with 0 kinetic energy.

Time-optimal Bang-Bang Control

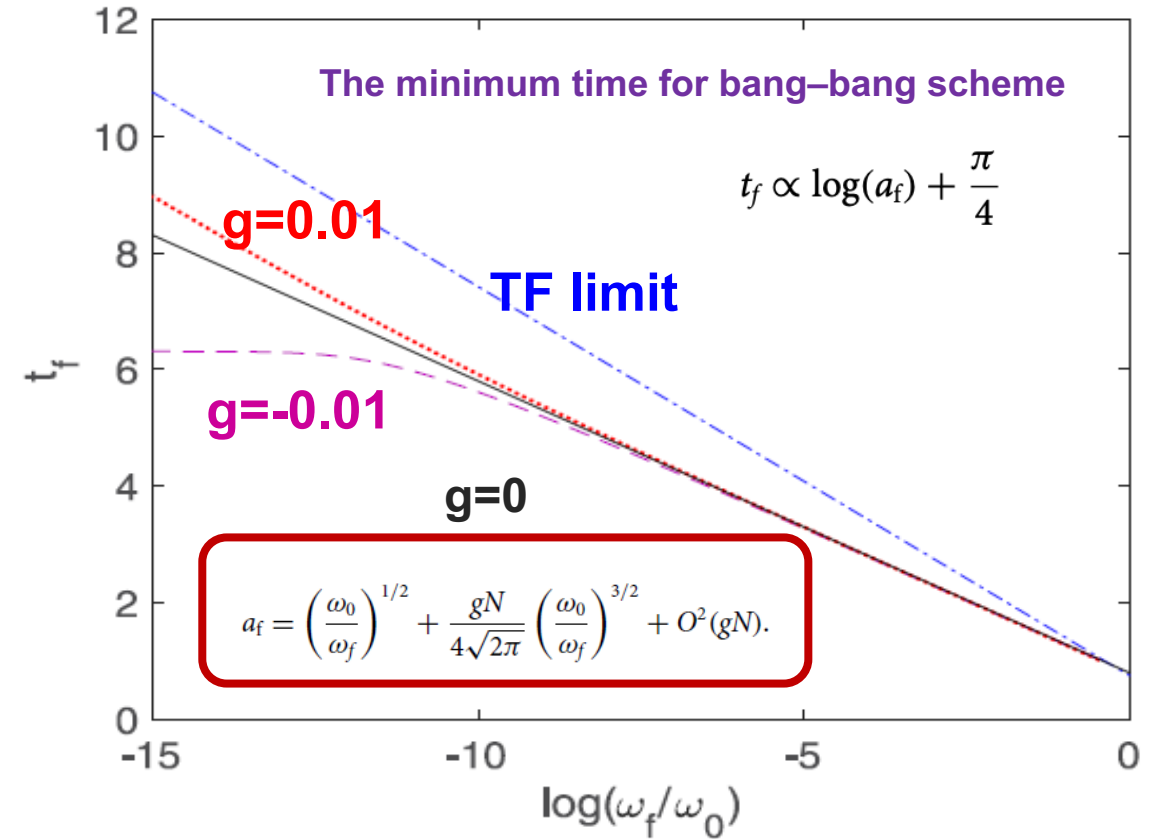
$$J = \int_0^{t_f} dt = t_f.$$

Chaos 30, 053131 (2020)



$$\dot{x}_1 = x_2,$$

$$\dot{x}_2 = -ux_1 + \frac{1}{x_1^3} + \frac{gN}{\sqrt{2\pi}} \frac{1}{x_1^2},$$



Fast Non-adiabatic Soliton Compression

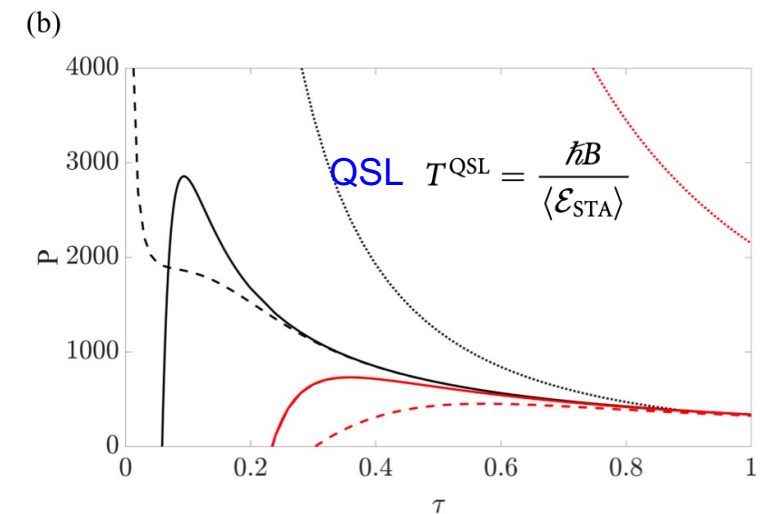
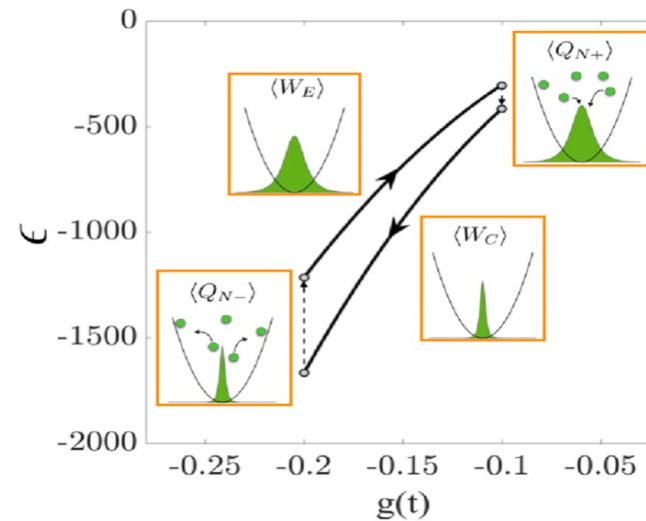
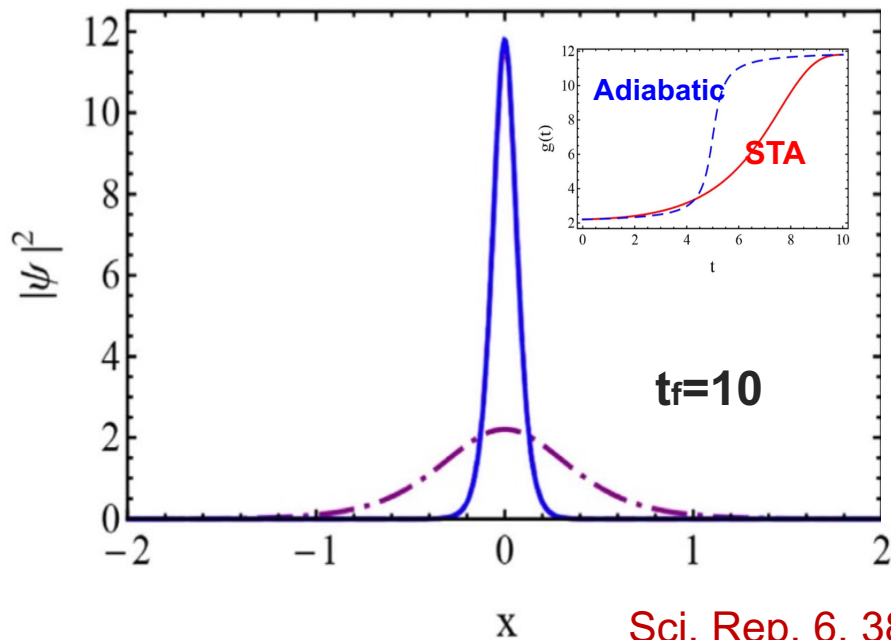
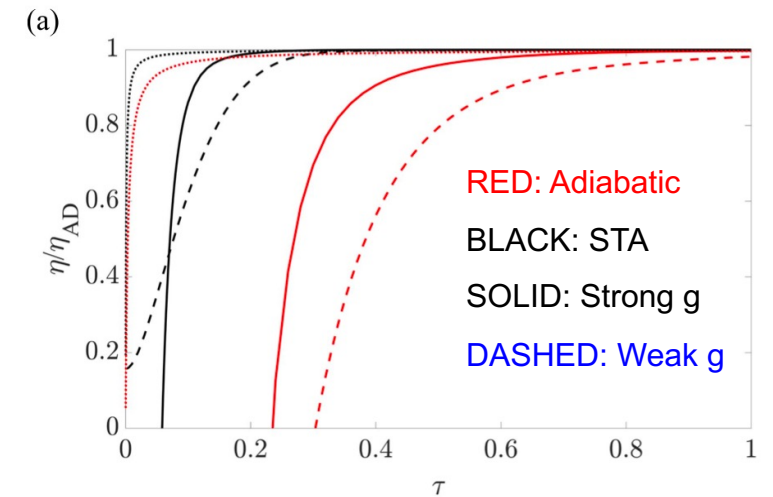
By choosing ansatz for bright soliton

$$\psi(x, t) = A(t) \operatorname{sech} \left[\frac{x}{a(t)} \right] e^{ib(t)x^2}$$

Ermakov-like Equation

$$\ddot{a} + \omega^2 a(t) = \frac{4}{\pi^2 a^3(t)} + \frac{2g(t)}{\pi^2 a^2(t)}$$

New J. Phys. 20, 015005 (2018)



Sci. Rep. 6, 38258 (2016) **Stronger non-linearities lead to a better overall performance**

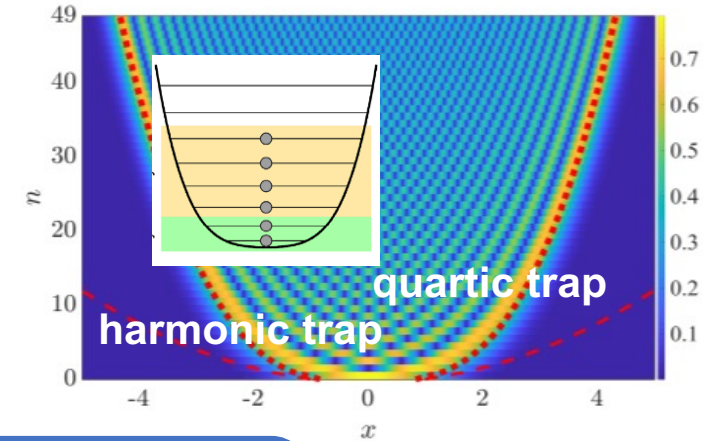
Arbitrary Power-law Potential

Lagrange density

$$\mathcal{L} = \frac{i}{2} \left(\frac{\partial \psi}{\partial t} \psi^* - \frac{\partial \psi^*}{\partial t} \psi \right) - \frac{1}{2} \left| \frac{\partial \psi}{\partial x} \right|^2 - \frac{\lambda(t)}{2} [x - x_0(t)]^{2q} |\psi|^2$$

Excited state is chosen as Ansatz

$$\psi_n(x, t) = A_n \exp \left[\frac{-x^2}{2a_n^2(t)} + ib(t)x^2 \right] H_n \left(\frac{x}{a_n(t)} \right)$$



The variational approach gives the following coupled differential equations:

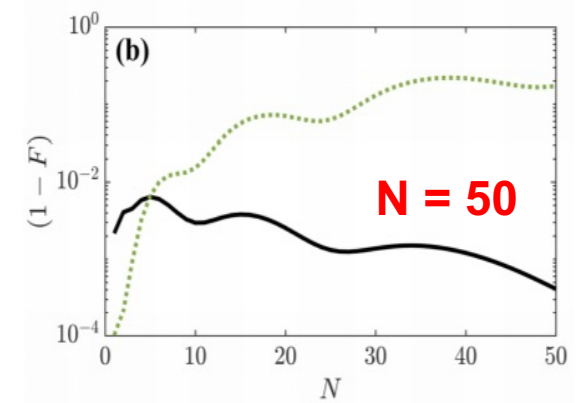
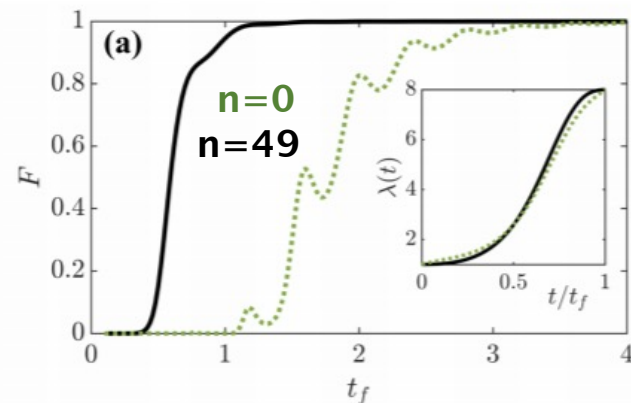
$$\ddot{a} + \frac{2\lambda(t)}{(2n+1)a} \sum_{k=0}^q k C(n) = \frac{1}{a^3},$$

$$\ddot{\xi} - \lambda(t) \sum_{k=0}^q \frac{q-k}{x_0 - \xi} C(n) = 0.$$

q=2

$$\ddot{a}_n(t) + \frac{3(2n^2 + 2n + 1)a_n^3(t)\lambda(t)}{2n + 1} = \frac{1}{a_n^3(t)}$$

$$C(n) = \frac{2^n}{n!} \sum_j \binom{n}{j}^2 \frac{j!}{2^{j(s+j)!}} \sum_{k=0}^q \binom{2q}{2k} (x_0 - \xi)^{2q-2k} \frac{2k! a^{2k}}{2^{2k}}.$$



Time-dependent 1-D GP equation with **harmonic potential**

Lagrange density

$$\mathcal{L} = - \left[\partial_t \phi + \frac{1}{2} (\nabla \phi)^2 + \frac{1}{8} \left(\frac{\nabla n}{n} \right)^2 + V(x, t) + gn \right] n$$

Madelung transformation

$$\psi = \sqrt{n(x, t)} e^{i\phi(x, t)}$$

Hydrodynamic equation:

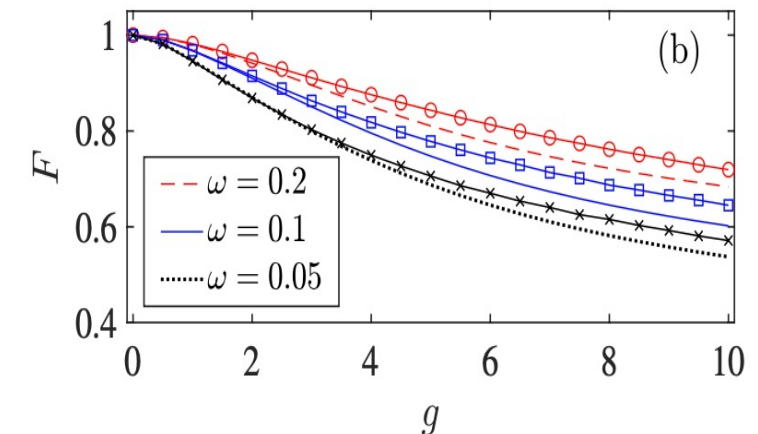
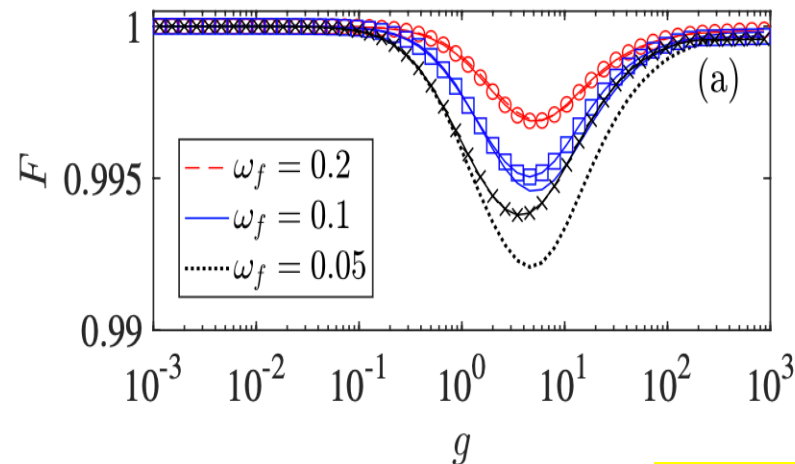
$$\frac{\partial n}{\partial t} + \frac{\partial (n \nabla \phi)}{\partial x} = 0,$$

$$\frac{\partial (\nabla \phi)}{\partial t} + \partial_x \left(P(x, t) + \frac{1}{2} v^2 + V(x, t) + gn \right) = 0,$$

Modified Ermakov equation connecting from noninteracting to TF limit

$$\ddot{a} + \omega^2(t)a = \frac{A}{a^3} + \frac{B}{a^2}$$

$$A = \frac{P(0, 0) - E_k^0}{E_v^0}, \quad B = \frac{gn(0, 0) - E_{int}^0}{E_v^0}$$



See the talk by Chinmayee Mishra

OUTLINE

1. Introduction

2. Trap Expansion

3. SOC Spin-1 BECs

4. Application to cQED

5. Conclusion & Outlook

SOC BEC

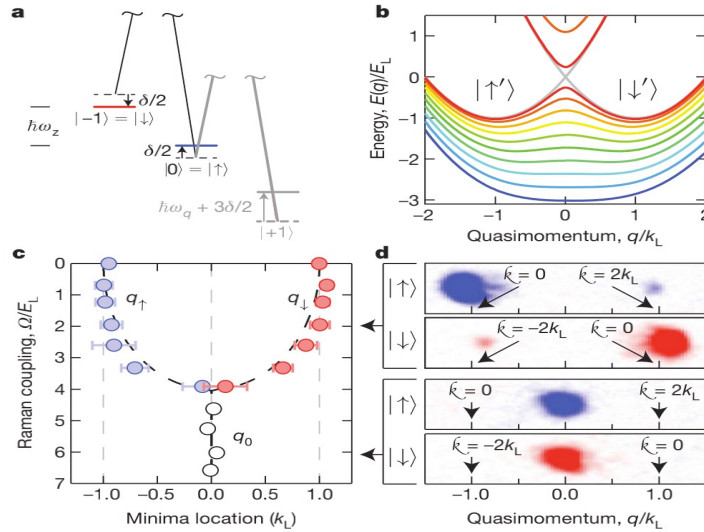
at single particle level

The Hamiltonian for spin-1 SOC BEC is described by

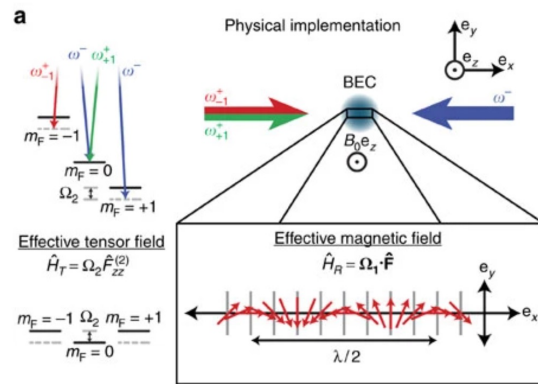
$$H = \frac{p_x^2}{2m} + \frac{1}{2}m\omega^2[x - x_0(t)]^2 + \alpha(t)p_x F_z + \hbar\Omega F_x.$$

Raman-induced SOC

In absence of the transverse potential ($\Omega = 0$)



Nature 471, 83 (2011)



Nat. Commun. 7, 10897 (2016)

Unitary operator: $U(t) = U_o(t)U_s(t)$ $\left\{ \begin{array}{l} U_o(t) = e^{-i\phi_{x_0}(t)} e^{-ix_c(t)p/\hbar} e^{im\dot{x}_c(t)x/\hbar} \\ U_s(t) = e^{-i\phi_\beta(t)} e^{-i\phi(t)F_z} e^{-im\beta_c(t)x F_z/\hbar} e^{-i\beta_c(t)p F_z/(\hbar\omega^2)} \end{array} \right.$

Unitary transformation: $H_0 = U(t)H(t)U^\dagger(t) - i\hbar\dot{U}(t)U^\dagger(t) = \frac{p^2}{2m} + \frac{1}{2}m\omega^2 x^2$

Spin rotation phase: $\phi(t) = -\frac{m}{\hbar} \int_0^t \dot{\beta}_c(\tau)x_0(\tau)d\tau$

Inverse engineering

We can obtain auxiliary differential equations:

$$\left\{ \begin{array}{l} \ddot{x}_c(t) + \omega^2 [x_c(t) - x_0(t)] = 0 \\ \ddot{\beta}_c(t) + \omega^2 [\beta_c(t) - \beta(t)] = 0 \end{array} \right.$$

The time evolution of the state:

$$|\Psi(t)\rangle = \mathcal{U}(t)e^{-iH_0t/\hbar}\mathcal{U}^\dagger(0)|\Psi(0)\rangle$$

$$|\Psi_{ms}(0)\rangle = \mathcal{U}(0)|\psi_n\rangle|\chi_s\rangle$$



$$|\Psi_{ns}(t)\rangle = e^{-i\omega_n t}\mathcal{U}(t)|\psi_n\rangle|\chi_s\rangle$$

Fast transport with spin flip

$$x_c(0) = 0, \quad \dot{x}_c(0) = 0, \quad \ddot{x}_c(0) = 0, \\ x_c(t_f) = d, \quad \dot{x}_c(t_f) = 0, \quad \ddot{x}_c(t_f) = 0.$$

$$\alpha_c(0) = \dot{\alpha}_c(0) = \ddot{\alpha}_c(0) = 0, \\ \alpha_c(t_f) = \dot{\alpha}_c(t_f) = \ddot{\alpha}_c(t_f) = 0,$$

$$\phi(t_f) = -\frac{m}{\hbar} \int_0^{t_f} \dot{\alpha}_c(\tau)x_0(\tau)d\tau = \pi,$$

Splitting with static trap

$$\alpha_c(0) = 0, \quad \dot{\alpha}_c(0) = 0, \quad \ddot{\alpha}_c(0) = 0, \\ \alpha_c(t_f) = 0, \quad \dot{\alpha}_c(t_f) = \omega^2 d, \quad \ddot{\alpha}_c(t_f) = 0.$$

Fast transport with spin flip

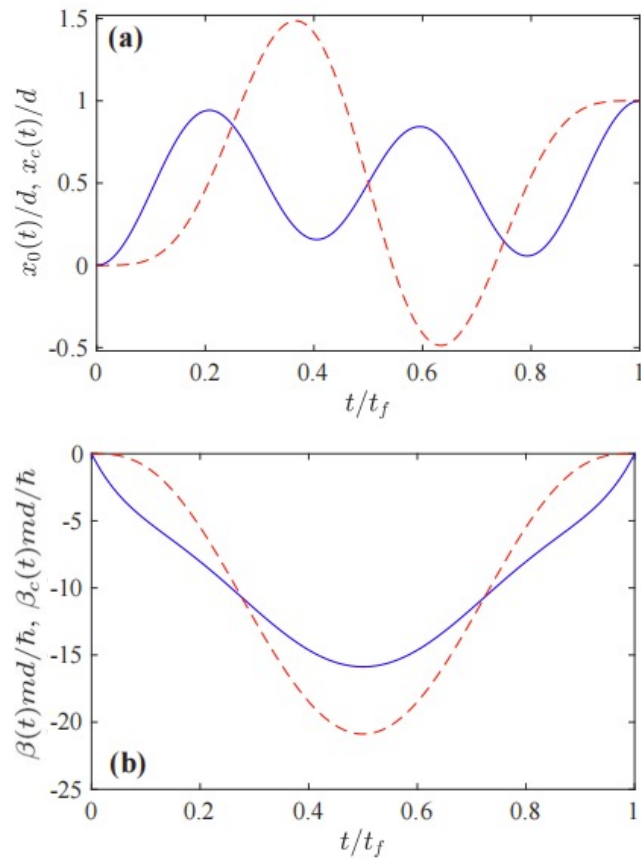


FIG. 1. (a) Dependence of the trap position $x_0(t)/d$ (solid blue line) and the center of mass $x_c(t)/d$ (dashed red line) of atoms on time t/t_f . (b) Dependence of the SOC strength $\beta(t)md/\hbar$ (solid blue line) and the auxiliary parameter $\beta_c(t)md/\hbar$ (dashed red line) on time t/t_f . All quantities are dimensionless. The parameters $t_f = 10$ and $d = 10$.

Initial state:

$$|\Psi(x, 0)\rangle = \frac{1}{2} (1, \sqrt{2}, 1)^T \otimes |\psi(x, 0)\rangle,$$

$$|\psi(x, 0)\rangle = \left(\frac{1}{\pi a^2}\right)^{1/4} \exp\left[-\frac{x^2}{2a^2}\right].$$

Final state:

$$|\Psi(x, t_f)\rangle = \frac{1}{2} (1, -\sqrt{2}, 1)^T \otimes |\psi(x, t_f)\rangle,$$

$$|\psi(x, t_f)\rangle = \left(\frac{1}{\pi a^2}\right)^{1/4} \exp\left[-\frac{(x-d)^2}{2a^2}\right].$$

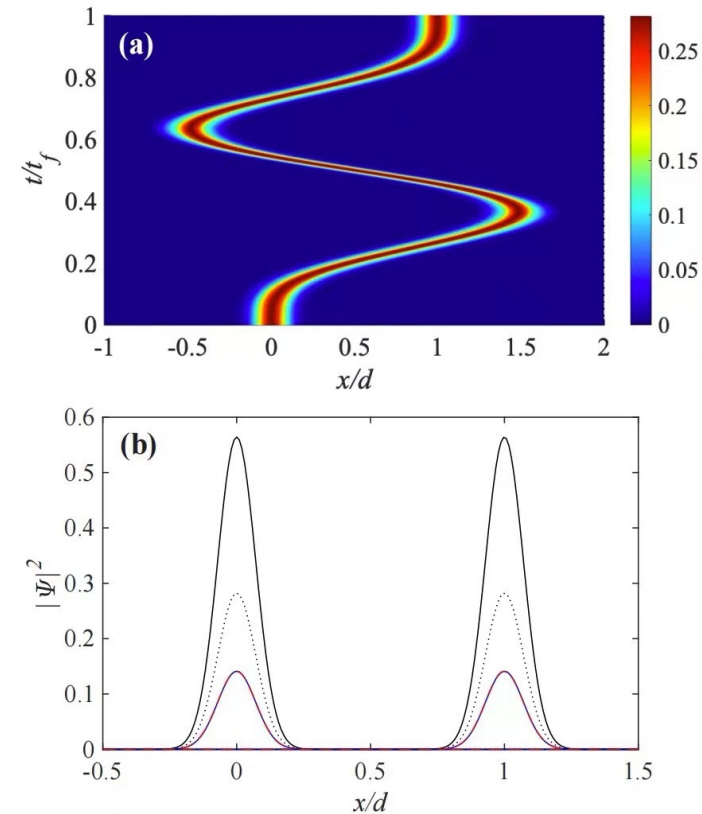


FIG. 2. (a) Depicts the propagation contour map of wave packets during the fast transport process designed using the inverse engineering method. (b) Illustrates the density distribution of the total wave function $|\Psi(x, t)|^2$ (black line) at $t = 0$ and $t = t_f$, along with the density distribution of the three spin components $|\Psi_{1,0,-1}(x, t)|^2$, denoted by blue solid line, black dotted line, and red dashed line, respectively.

Spin rotation

$$v = \frac{i}{\hbar} [H, x] = \frac{p}{m} + \alpha(t)F_z$$

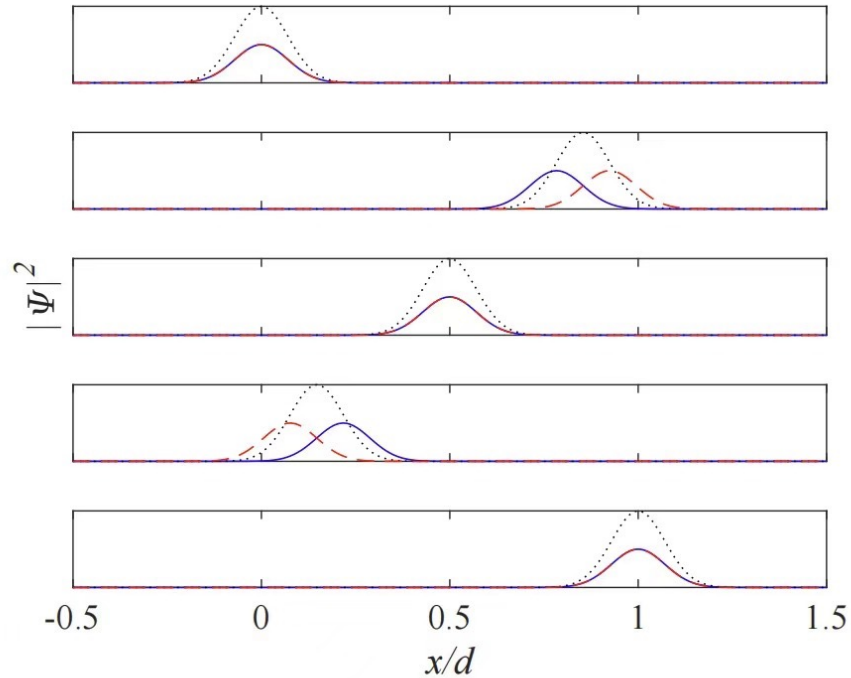


FIG. 3. Time evolution of the wave packets with spin-up (solid blue line), spin-zero (dotted black line) and spin-down (dashed red line) components at different times: $t = 0, t_f/4, t_f/2, 3t_f/4, t_f$.

$$\rho(t) = |\Psi(x, t)\rangle\langle\Psi(x, t)|,$$

$$\rho_{ij}(t) = \int \Psi_i(x, t)\Psi_j^*(x, t)dx \quad (i, j = 1, 0, -1).$$

$$\langle F_i \rangle = \text{tr}(F_i \rho) \quad (i = x, y, z)$$

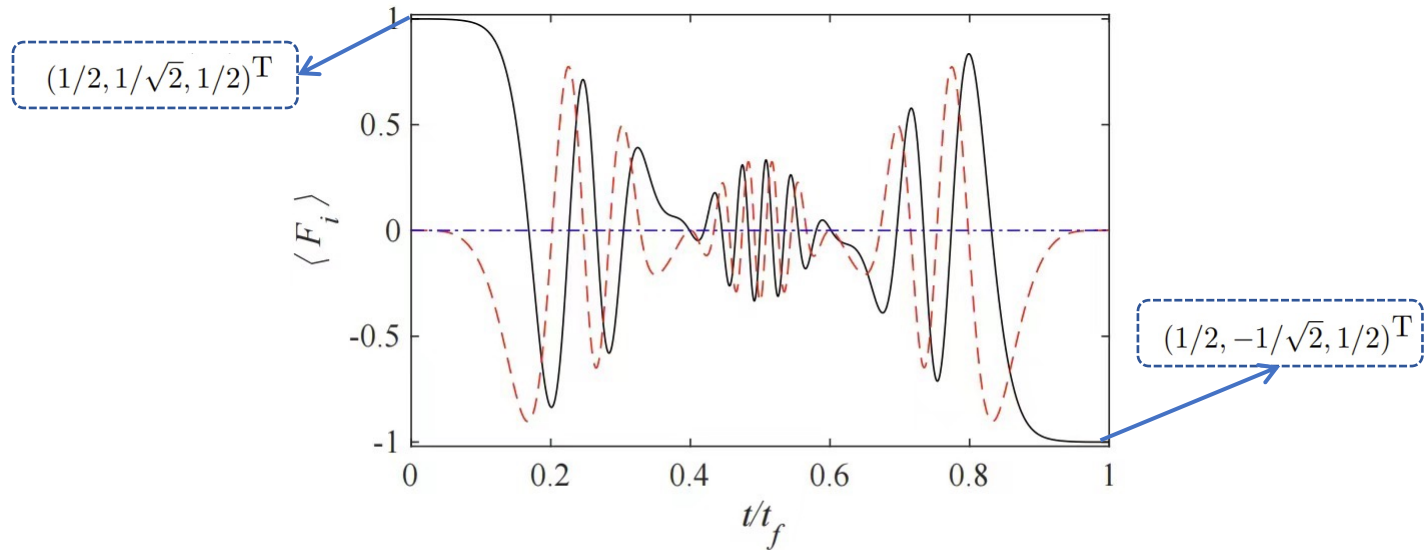


FIG. 4. Time evolution of spin components $\langle F_i \rangle$ during the fast transport, representing $\langle F_x \rangle$ (solid black line), $\langle F_y \rangle$ (dashed red line), and $\langle F_z \rangle$ (dotted-dash blue line).

Fast wave-packet splitting (preparation of spin-dependent coherent state)

The single particle Hamiltonian is reduced to

$$H = p_x^2/2m + m\omega^2 x^2/2 + \alpha(t)p_x F_z.$$



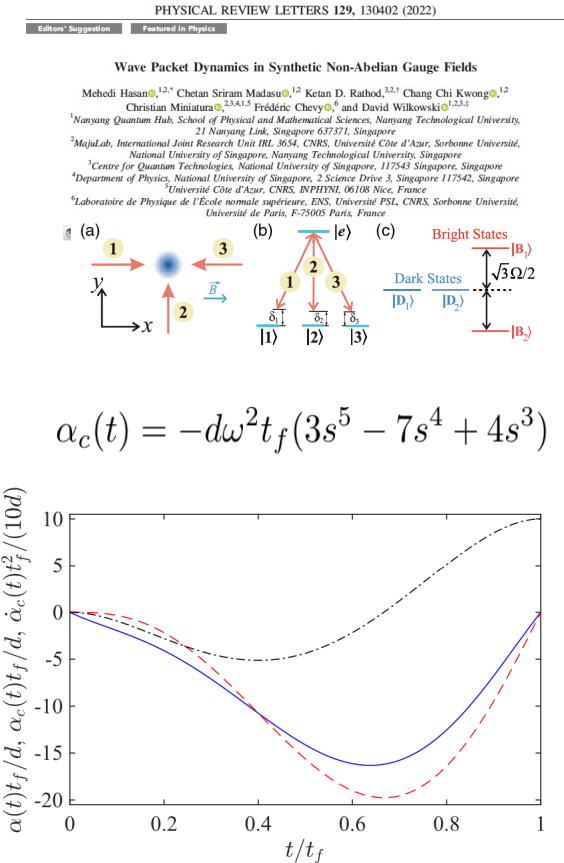
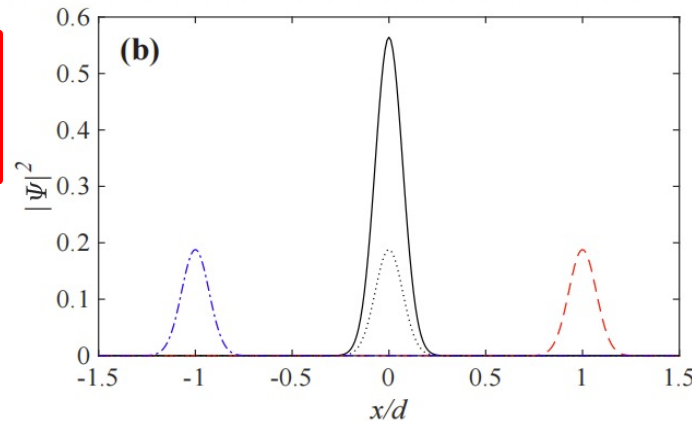
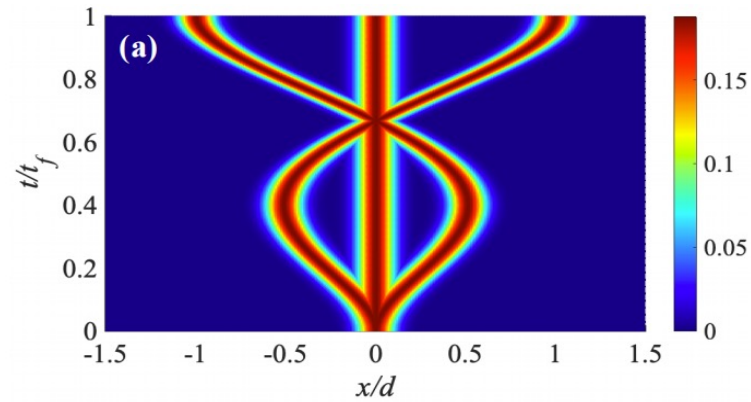
$$|\Psi(t)\rangle = e^{i\phi_\alpha} e^{[\beta(t)a^\dagger - \beta^*(t)a]F_z} e^{-iH_0 t/\hbar} |\Psi(0)\rangle$$

Displacement operator

where

$$\beta(t) = \sqrt{\frac{m\omega}{2\hbar}} \left[\frac{\dot{\alpha}_c(t)}{\omega^2} - i \frac{\alpha_c(t)}{\omega} \right].$$

arXiv: 2405.10727, accepted by Phys. Rev. A

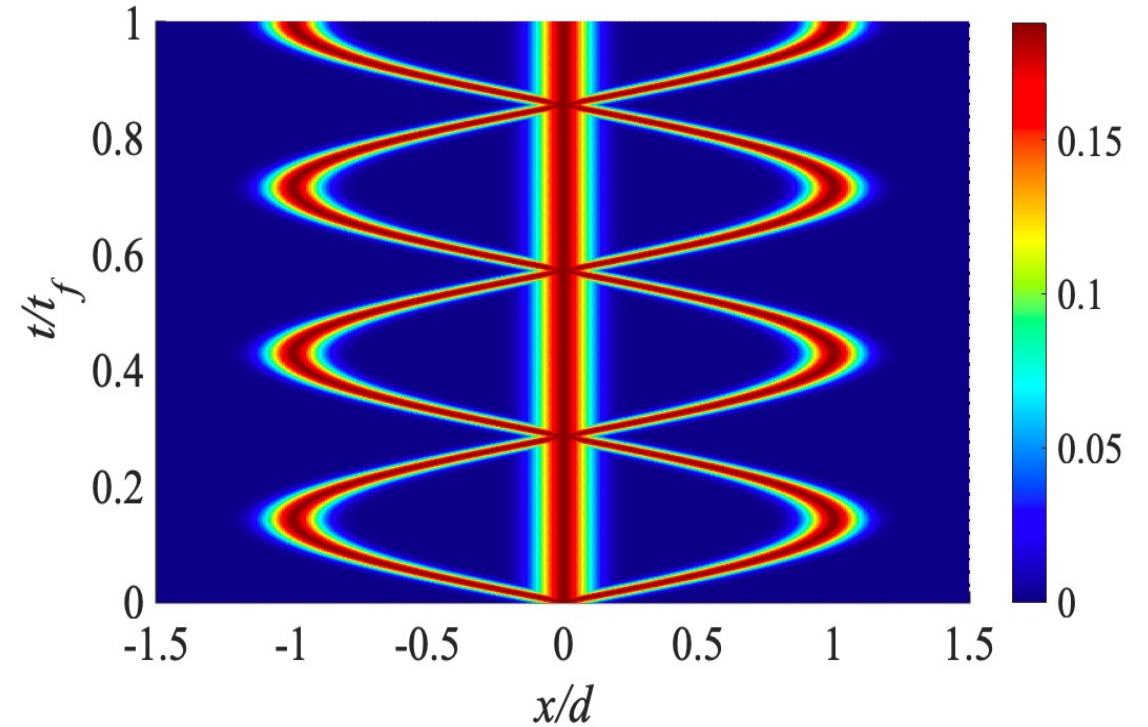
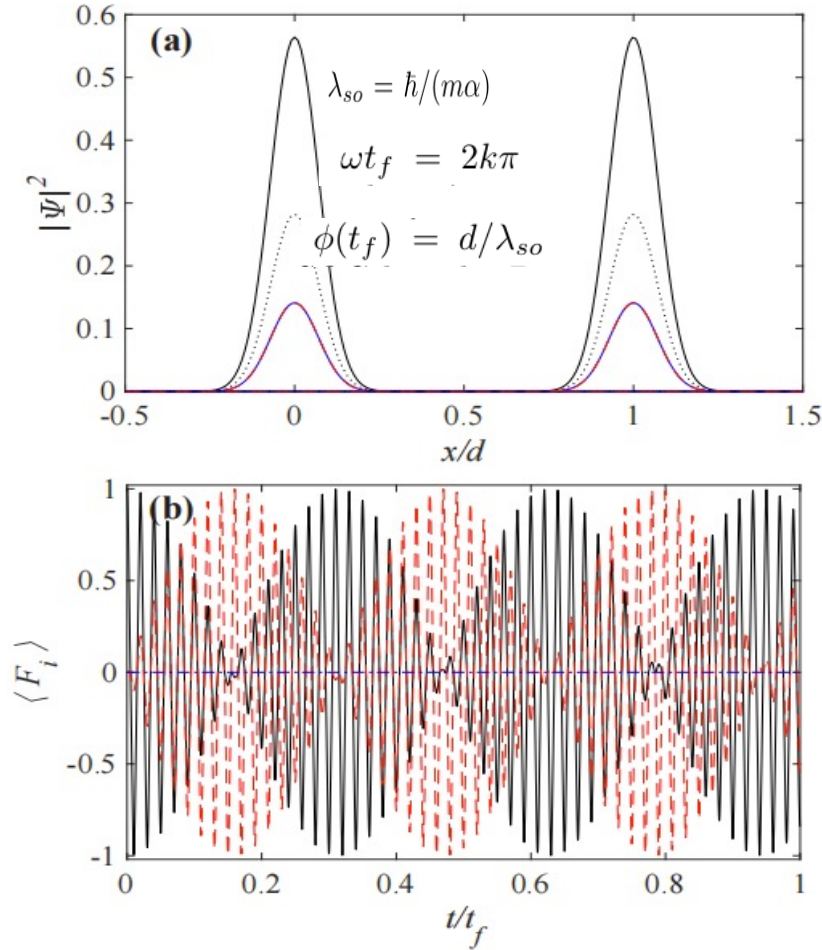


$$|\Psi(x, 0)\rangle = \frac{\sqrt{3}}{3} \begin{pmatrix} 1, 1, 1 \end{pmatrix}^T \otimes \left(\frac{1}{\pi a^2} \right)^{1/4} \exp \left[-\frac{x^2}{2a^2} \right]$$

$$|\Psi_i(x, t_f)\rangle = \frac{\sqrt{3}}{3} \left(\frac{1}{\pi a^2} \right)^{1/4} \exp \left[-\frac{(x^2 - x_i^2)}{2a^2} \right]$$

Constant SOC strength and velocity

$$x_c(t) = x_0(t) = dt/t_f$$



$$\langle x_{\pm}(t_f) \rangle = \pm \frac{\dot{\alpha}_c(t_f)}{\omega^2} = \pm \frac{\alpha \sin(\omega t_f)}{\omega}.$$

$$\phi(t_f) = -\frac{md\alpha}{\hbar\omega t_f} [\sin(\omega t_f) - \omega t_f \cos(\omega t_f)].$$

$$\langle v_{\pm}(t_f) \rangle = \pm \frac{\ddot{\alpha}_c(t_f)}{\omega^2} = \pm \alpha \cos(\omega t_f).$$

Nonlinear interaction

$$c_2/c_0 = -0.005$$

GP equation:

$$i\hbar \frac{\partial \Psi(x,t)}{\partial t} = (H + H_{int})\Psi(x,t)$$

$$H_{int} = \begin{pmatrix} \Gamma_1 & 0 & 0 \\ 0 & \Gamma_0 & 0 \\ 0 & 0 & \Gamma_{-1} \end{pmatrix}$$

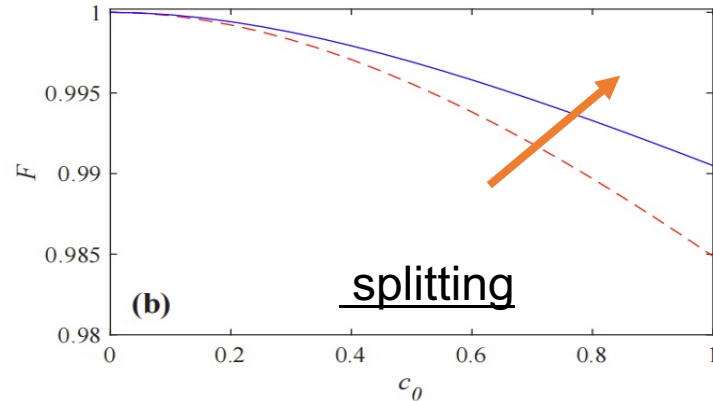
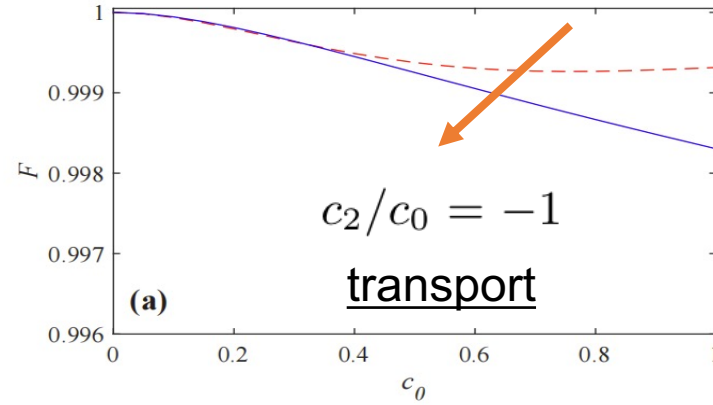
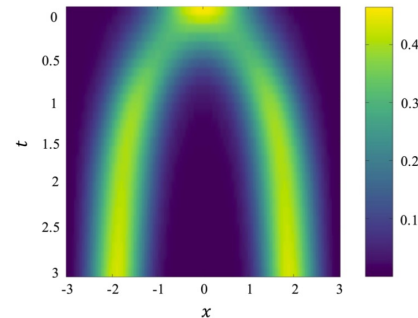
$$\Gamma_{\pm} = (c_0 + c_2)(|\psi_1|^2 + |\psi_0|^2 + |\psi_{-1}|^2) - 2c_2|\psi_{\mp}|^2$$

$$\Gamma_0 = (c_0 + c_2)(|\psi_1|^2 + |\psi_0|^2 + |\psi_{-1}|^2) - c_2|\psi_0|^2$$

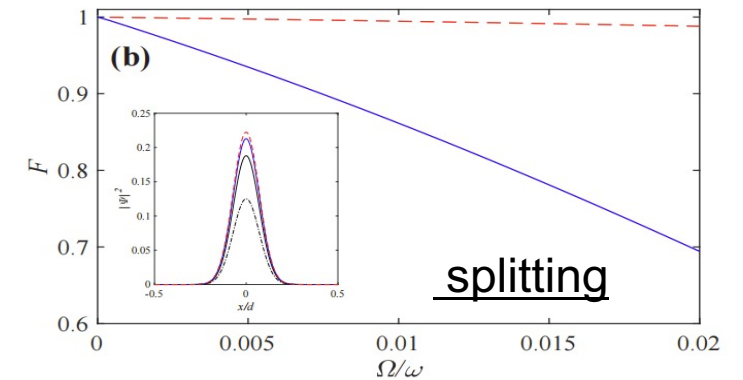
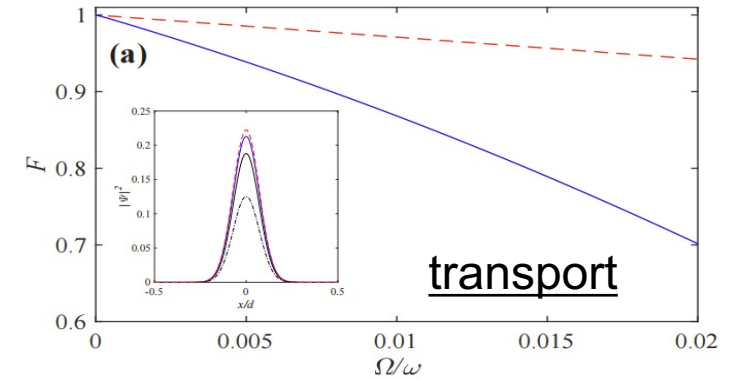
Fidelity:

$$F = \left| \langle \Psi(x, t_f) | \tilde{\Psi}(x, t_f) \rangle \right|^2$$

Potential applications:
Interferometry



$$c_0 = 0.05, c_2/c_0 = -0.005, \Omega/\omega = 0.02.$$



Time-imaginary (blue) and Gaussian (red)

OUTLINE

1. Introduction

2. Trap Expansion

3. SOC Spin-1 BECs

4. Application to cQED

5. Conclusion & Outlook

Qubit Readout by Tunable Longitudinal Coupling

LC oscillator longitudinally coupled to a two-level with time-dependent coupling

$$\mathcal{H} = \frac{\omega_q}{2} \sigma^z + \omega_r \hat{a}^\dagger \hat{a} + g_z(t) \sigma^z (\hat{a}^\dagger + \hat{a}).$$

The dynamical equation of the cavity field regarding losses reads

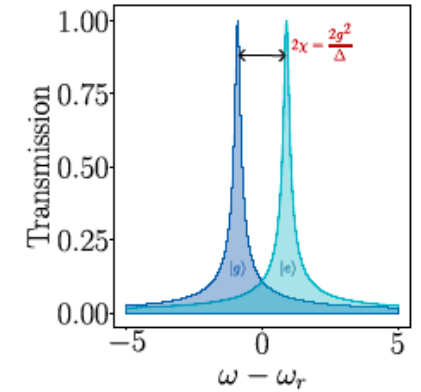
$$\dot{\hat{a}} = i \tilde{g}_z(t) \sigma^z - \kappa \hat{a} / 2 - \sqrt{\kappa} \hat{a}_{in},$$

κ is the decay rate of the LC oscillator.

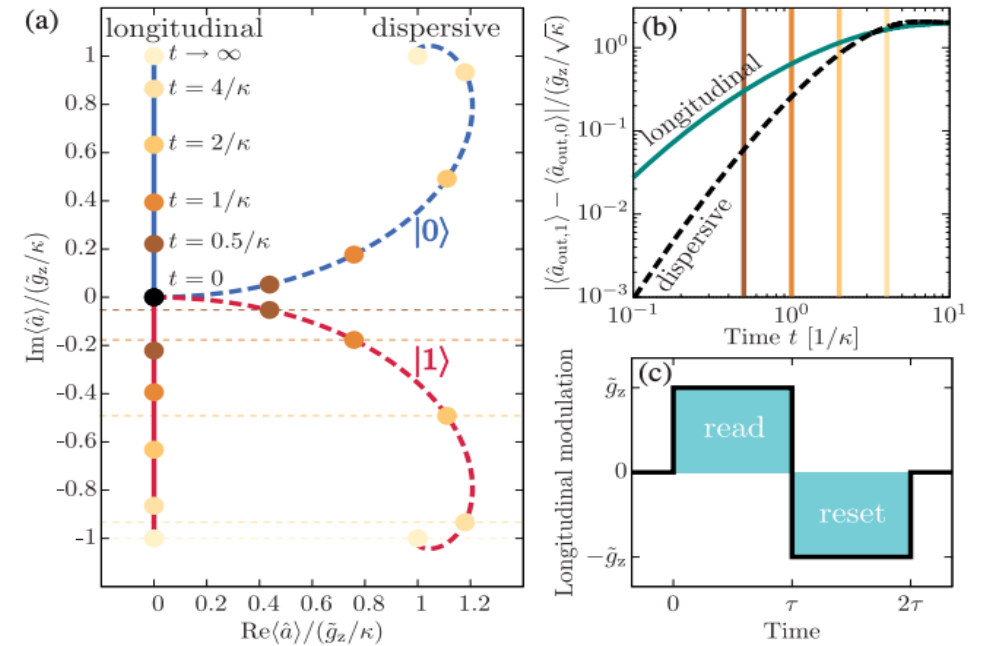
The equation of motion for the expectation value

$$\langle \hat{a}(t) \rangle = -i \langle \sigma^z \rangle e^{-\kappa t / 2} \int_0^t g_c(s) e^{\kappa s / 2} ds.$$

for the cavity initialized in its vacuum state.



$$\langle \hat{a}_{out,\ell}(t) \rangle = \sqrt{\kappa} \langle \hat{a}(t) \rangle$$



$$d = |\langle \hat{a}_{out,e}(t) \rangle - \langle \hat{a}_{out,g}(t) \rangle|$$

PRL 115, 203601 (2015)

Inverse engineering

The effective Hamiltonian reads

$$\hat{H}_{\text{eff}} = \mathcal{V}^\dagger(t) \mathcal{H} \mathcal{V}(t) - i \partial_t [\mathcal{V}^\dagger(t)] \mathcal{V}(t) \equiv \omega_r a^\dagger a + \frac{\omega_q}{2} \sigma^z$$

with the unitary transformation

$$\hat{\mathcal{V}}(t) = e^{i\theta(t)} \exp \left[-i \frac{\dot{g}_c(t)}{\omega_r^2} \sigma^z (a^\dagger + a) \right] \exp \left[-\frac{g_c(t)}{\omega_r} \sigma^z (a^\dagger - a) \right]$$

when the conditions

$$\dot{\theta}(t) = \frac{\dot{g}_c^2(t)}{\omega_r^3} - \frac{g_c^2(t)}{\omega_r} + \frac{2g_c(t)g_z(t)}{\omega_r},$$

$$\ddot{g}_c(t) + \omega_r^2 [g_c(t) - g_z(t)] = 0.$$

are satisfied

$$\mathcal{L}_g(t) = \frac{\dot{g}_c^2(t)}{\omega_r^3} - \frac{g_c^2(t)}{\omega_r} + \frac{2g_c(t)g_z(t)}{\omega_r}.$$

$$g_c(0) = 0; g_c(t_f) = 0,$$

$$\dot{g}_c(0) = \ddot{g}_c(0) = \dot{g}_c(t_f) = \ddot{g}_c(t_f) = 0.$$

$$\int_0^{t_f} g_c(s) ds = g_{z0} \pi / (2\kappa).$$

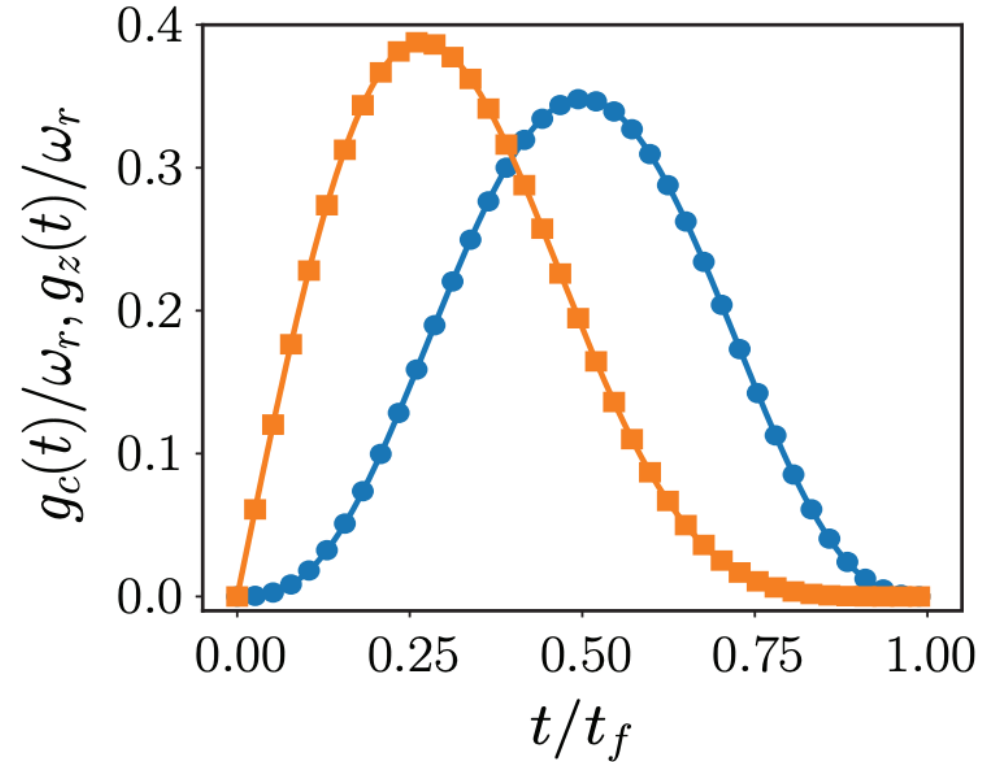
final cavity displacement

$$\kappa/2\pi = 1 \text{ MHz}, g_{z0}/2\pi = 21 \text{ MHz}, \omega_r/2\pi = 6.6 \text{ GHz}:$$

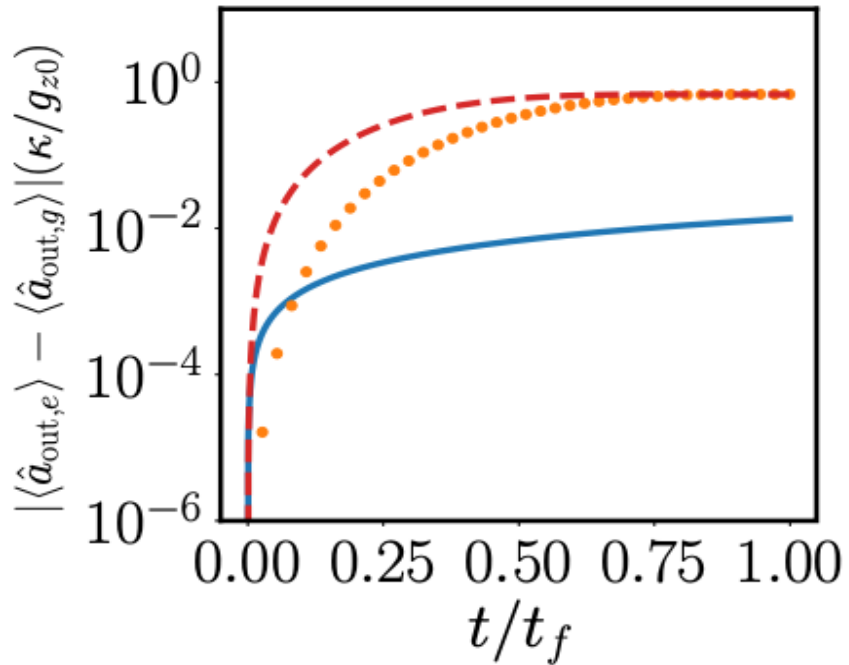
$$t_f = \pi / (100\kappa)$$

$$g_c(t) = -\frac{70\pi g_{z0} t^3 (t - t_f)^3}{\kappa t_f^7}. \text{ Blue}$$

$$g_c(t) = \frac{3g_{z0}\pi^2}{2\kappa t_f} \sin\left(\frac{\pi t}{2t_f}\right) \cos^5\left(\frac{\pi t}{2t_f}\right). \text{ Orange}$$



Cavity displacement and Signal to noise ratio (SNR)



STA: polynomial (orange) and trigonometric (red)
conventional sinusoidal modulation (blue)

- Homodyne operator

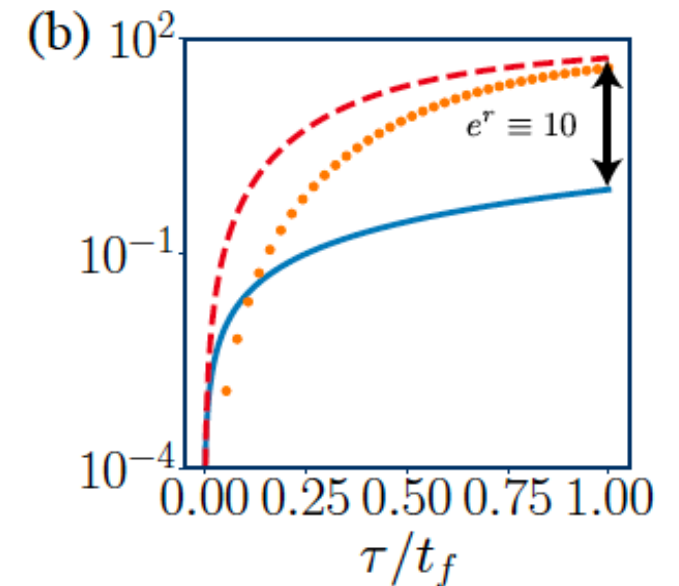
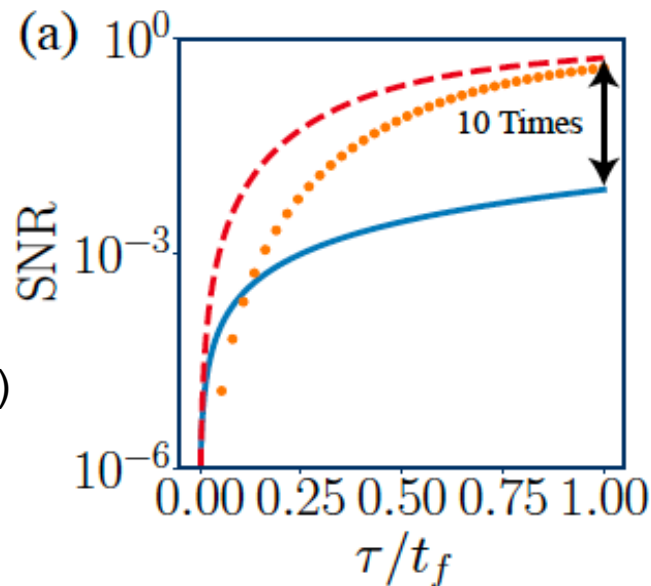
$$\hat{\mathcal{M}}(\tau) = \sqrt{\kappa} \int_0^\tau ds (a_{\text{out}}^\dagger(t) \exp(i\phi) + a_{\text{out}}(t) \exp(-i\phi)).$$

- Fluctuation of the operator

$$\hat{\mathcal{M}}_{\text{Ne}}(\tau) = \hat{\mathcal{M}}_e(\tau) - \langle \hat{\mathcal{M}}_e(\tau) \rangle.$$

- SNR

$$\text{SNR}(\tau) = \frac{|\langle \hat{\mathcal{M}}_e \rangle - \langle \hat{\mathcal{M}}_g \rangle|}{\sqrt{\langle \hat{\mathcal{M}}_{\text{Ne}}^2 \rangle + \langle \hat{\mathcal{M}}_{\text{Ng}}^2 \rangle}}.$$



Larger value of the SNR at times shorter than the coherence times.

$$\theta = \pi/4 \text{ and } r = 20 \text{ (dB)} \equiv e^{2r} = 100$$

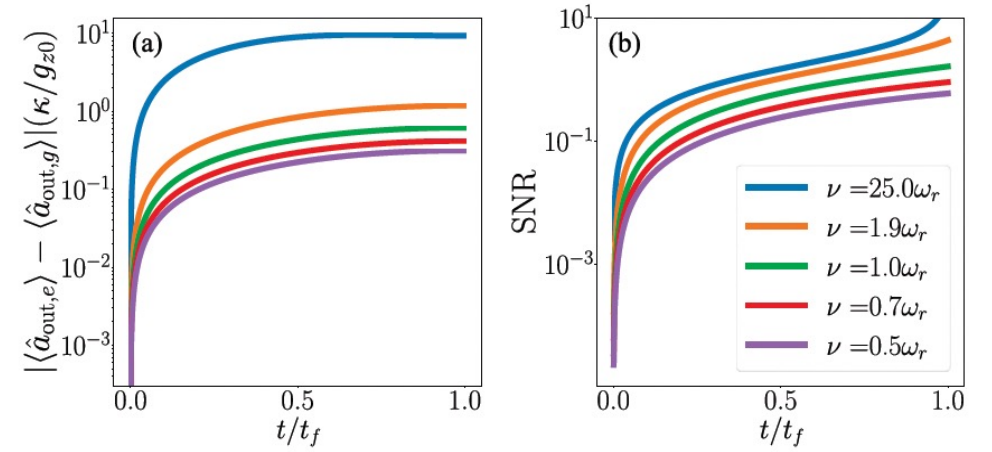
Floquet engineering

We propose a driven Hamiltonian

$$\hat{\mathcal{H}}_{\text{FE}}(t) = \Omega\nu \sin(\nu t)(\hat{\sigma}^z + a^\dagger a) + \lambda(t)\hat{\sigma}^z(\hat{a}^\dagger + \hat{a}),$$

In the Floquet frame through the transformation

$$\hat{U}(t) = \exp \left[i\Omega \cos(\nu t)(\hat{\sigma}^z + \hat{a}^\dagger \hat{a}) \right].$$



$$\tilde{\mathcal{H}}_{\text{FE}}(t) = \lambda(t)\hat{\sigma}^z(\hat{a}^\dagger e^{-i\Omega \cos \nu t} + \hat{a} e^{i\Omega \cos \nu t}).$$

Floquet modulation circumvents the implementation problem of the counter-diabatic term.

We compare the averaged Floquet Hamiltonian with the counter-diabatic term

$$\tilde{\mathcal{H}}_{\text{FE}}^{(0)}(t) = \frac{1}{T} \int_0^T \lambda(t)\hat{\sigma}^z(\hat{a}^\dagger e^{-i\Omega \cos \nu t} + \hat{a} e^{i\Omega \cos \nu t}) dt = -i \frac{\dot{g}_z(t)}{\omega_r} \sigma^z (a^\dagger - a).$$

$$\frac{1}{T} \int_0^T \lambda(t) e^{-i\Omega \cos \nu t} dt = -i \frac{\dot{g}_z(t)}{\omega_r}, \quad \frac{1}{T} \int_0^T \lambda(t) e^{i\Omega \cos \nu t} dt = i \frac{\dot{g}_z(t)}{\omega_r}.$$

PRL 123, 090602 (2019)

PR Appl. 18, 034010 (2022)

$$\mathcal{H}_{\text{FE}}(t) = \Omega\nu \sin(\nu t)(\sigma^z + a^\dagger a) + \frac{\dot{g}_z(t)}{\omega_r J_1(\Omega)} \cos(\nu t) \sigma^z (a^\dagger + a)$$

Controlled-Phase Gate

$$\mathcal{H}(t) = \omega_r \hat{a}^\dagger \hat{a} + \sum_{\ell=\{1,2\}} \left[\frac{\omega_{q,\ell}}{2} \hat{\sigma}_\ell^z + \lambda_\ell(t) \hat{\sigma}_\ell^z (\hat{a}^\dagger + \hat{a}) \right]$$

$\{|gg\rangle, |ge\rangle, |eg\rangle, |ee\rangle\}$

$$\text{CZ}(\Theta_{\ell,\ell'}) \equiv \begin{bmatrix} 1 & 0 & 0 & 0 \\ 0 & 1 & 0 & 0 \\ 0 & 0 & 1 & 0 \\ 0 & 0 & 0 & e^{i\Theta_{\ell,\ell'}} \end{bmatrix}$$

SM gate

Fast Multi-Partite State Generation

$$\mathcal{H}_n^m = \sum_n \frac{\Omega_n}{2} \sigma_n^x + \sum_m \omega_m a_m^\dagger a_m + \sum_{n,m} g_n^m(t) \sigma_n^x (a_m^\dagger + a_m),$$

a set of N 2-level systems coupled to M field modes

$$|\Psi(0)\rangle = |g\rangle \otimes_{m=1}^M |0\rangle_m$$

$$|\Psi(T)\rangle = \frac{1}{\sqrt{2}} \left[|e\rangle \otimes_{m=1}^M |\alpha_{\max}\rangle_m + |g\rangle \otimes_{m=1}^M |-\alpha_{\max}\rangle_m \right]$$

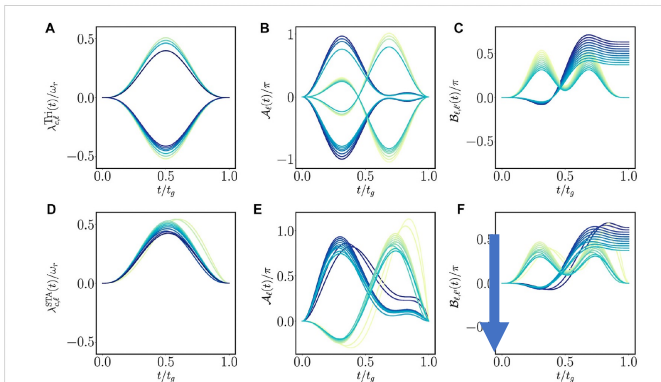


FIGURE 1 Modulation of coupling strength $\lambda_l(t)$ as a function of the normalized time t/t_g for different values of $\Theta_{\ell,\ell'} = (0, \pi/8)$ for (A) trigonometric and (D) STA modulation, and the parameter $A_l(t)$ as a function of the normalized time for different phases, where green and blue lines correspond to the real and imaginary parts of $A_l(t)$, respectively; see (B) trigonometric and (E) STA modulation. Finally, for the modulated phase $B_{\ell,\ell'}$ as a function of t/t_g for different final phases $\Theta_{\ell,\ell'}$, see (C) trigonometric and (F) STA modulation, where yellow and blue lines stand for real and imaginary parts, respectively. The simulations were performed using the practical parameters $\omega_{qr} = 2\pi \times 5.28$ GHz, $\omega_r = 2\pi \times 10$ GHz, and $t_g = 12\pi/\omega_r = 1.89$ ns.

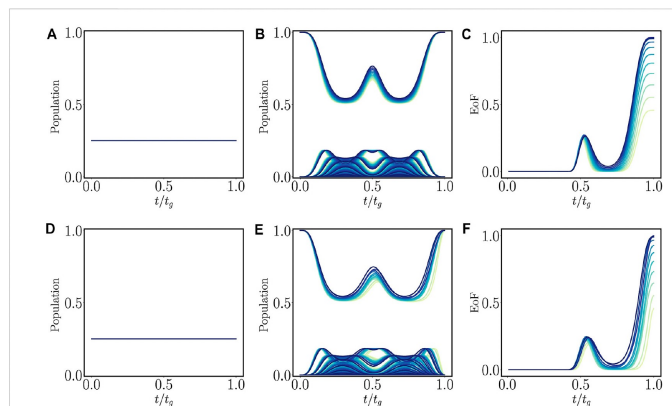
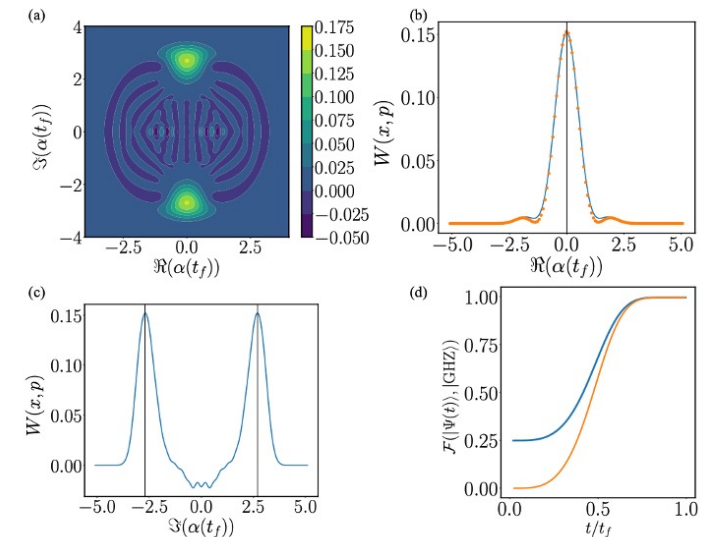


FIGURE 2 Population of the pair of two-level systems as a function of the normalized time t/t_g for different values of $\Theta_{\ell,\ell'} = (0, \pi/8)$ for (A) trigonometric and (D) STA modulation. Population evolution of the resonator as a function of the normalized time t/t_g for the (B) trigonometric and (E) STA modulation. Finally, EoF for the reduced density matrix consisting of the pair of two-level systems as a function of the normalized time t/t_g for the (C) trigonometric and (F) STA modulation. The parameters are the same as those in Figure 1.



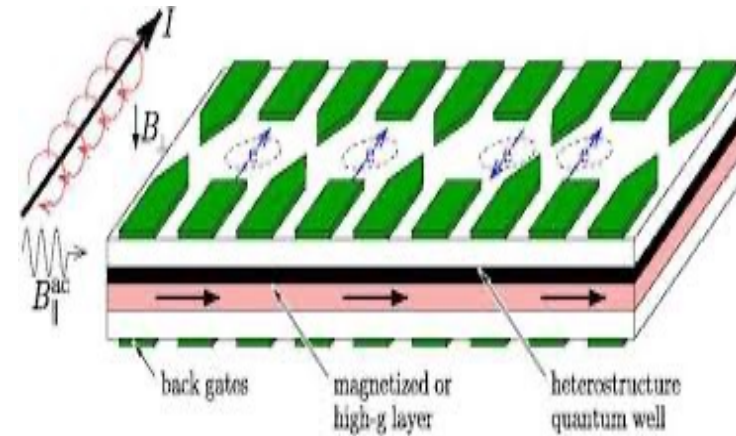
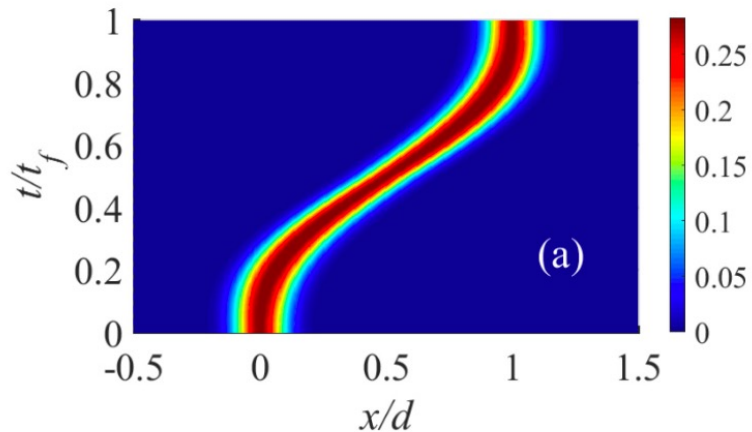
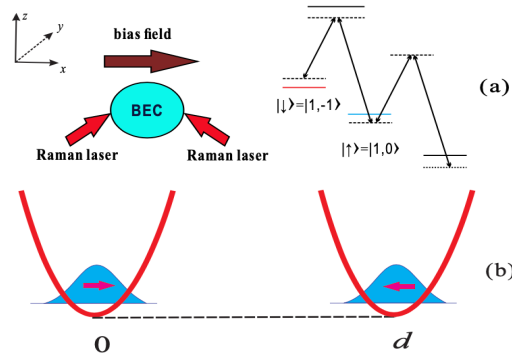
Take Home Message (Further work: Variational Approximation/Hydrodynamics for SOC BECs)

$$H = \frac{p^2}{2m} + \frac{1}{2}m\omega^2[x - x_0(t)]^2 + \alpha(t)p\sigma_z$$

$$\ddot{x}_c(t) + \omega^2[x_c(t) - x_0(t)] = 0,$$

$$\ddot{a}_c(t) + \omega^2[a_c(t) - \alpha(t)] = 0,$$

$$\phi_\sigma(t) = -\frac{m}{\hbar} \int_0^t \dot{a}_c(\tau)x_0(\tau) d\tau.$$



PRL 112, 150402 (2014).

PRA 97, 013631 (2018)

PRA in press (2024)

also applicable to cQED & QD

Schrödinger cat generation

Phys. Rev. B 96, 115308 (2017)

spin-to-charge conversion

Phys. Rev. B 98, 125411 (2018)

PHYSICAL REVIEW LETTERS

Highlights Recent Accepted Collections Authors Referees Search Press About

Fully Tunable Longitudinal Spin-Photon Interactions in Si and Ge Quantum Dots

Stefano Bosco, Pasquale Scarlino, Jelena Klinovaja, and Daniel Loss
Phys. Rev. Lett. 129, 066801 – Published 2 August 2022

QD with longitudinal coupling

Thank You for Your Attention!